ECOSYSTEMS: ECOLOGY AND DYNAMICS, 2021, Vol. 5, No. 3, P. 192-224

DYNAMICS OF ECOSYSTEMS AND THEIR COMPONENTS

UDC 556.383/388:504(571.1)

MODELING OF THE POLLUTED GROUNDWATER FLOW INTO CONFINED WATER IN THE FOREST ECOSYSTEMS BY THE EXAMPLE OF THE KALUGA REGION IN THE RADIOACTIVE CONTAMINATION ZONE[1]

© 2021. A.P. Belousova, E.E. Rudenko

Water Problems Institute of the Russian Academy of Sciences
Russia, 119333, Moscow, Gubkina Str., 3. E-mail: anabel@iwp.ru, belanna47@mail.ru

Received June 14, 2021. After revision August 30, 2021. Accepted September 01, 2021.

The purpose of this article is to study the migration processes of various pollutants, including radionuclides, from poorly sorbed to highly sorbed ones, in the groundwater and confined water, using the method of mathematical modeling. The object of the study is the part of the Kaluga Region that was affected by the accident at the Chernobyl Nuclear Power Plant the most.

The modeling of contamination processes in the groundwater and confined water in the radioactive contamination zone was carried out according to 3 scenarios of the development of such processes. We took into account various pollutants and mass transfer processes, using the mathematical MT3D program, and made a series of numerical experiments. Scenario 1) groundwater contamination with highly sorbed pollutants; scenario 2) contamination with highly sorbed pollutants and radioactive pollutants; scenario 3) contamination with poorly sorbed pollutants.

Besides, an unfavorable option for the ecological condition of confined waters was considered, due to the impervious horizon being insufficiently impermeable to the polluted waters, flowing from the aquifer. This situation was probably caused by the natural lithological structure (interlayers, sand lenses, sandy loams, insufficient depth) and industrial factors (poorly insulated holes, wells and other structures that open the aquifer). All the factors listed above are the "fast migration routes" that make it possible for a lot of pollutants to penetrate the confined aquifers, where the fresh water is contained.

To study the pollutants migration in the previously created MT3D model, we selected two profiles. They were located along the lines of groundwater flow, stretching from the watershed to the area of discharge, i.e. the rivers. The ecological situation was analyzed for 4 calculation periods of 30, 60, 100 and 300 years (to link it to the half-lives of radionuclides), for 4 coefficients of sorption distribution (C_d) of pollutants: 6, 26, 200 and 1000 l/kg for radionuclides with decay and other toxic, strongly sorbed pollutants without it; 0.5, 1.0 and 3.0 l/kg for poorly sorbed pollutants. We assessed the ecological situation in the first layer (groundwater), the second one (watershed layer and pore solutions) and the third one (confined water).

In addition, several spots were selected for the analysis of the ecological situation.

The modeling resulted in a comparison of all development scenarios of the pollution processes and analysis of the factors that determined them. In addition, we studied the capabilities of the process of pollutant diffusion and its impact on pollutant migration. Therefore, the main factors to form the processes of pollutant migration are their radioactive decay, their sorption characteristics, and the hydrodispersion of groundwater flows, which depends on the geological and hydrogeological conditions of the studied territory. Aside from this, diffusion plays an insignificant role in their migration as well.

Keywords: groundwater, confined water, migration processes modeling, pollutants, radionuclides, sorption, molecular diffusion, radioactive decay.

DOI: 10.24412/2542-2006-2021-3-192-224

[1] The study was funded by the Russian Foundation for Basic Research as part of the scientific project No. 20-55-S52003 "Ecological Security of Nuclear Power Plants in Normal and Emergency Situations, with an Assessment of the Uncertainty in the Disposal of Nuclear Waste and Reliability of Engineering Barrier Systems"; and the Government Contract, Program No. AAAA-A18-118022090104-8 "Modeling and Forecasting the Restoration Processes of Water and Ecosystems Quality under Various Scenarios of Climate Change and Anthropogenic Activities".

The object of our research is the confined waters in the territory of the Kaluga Region, Russia. The purpose is to apply the method of mathematical modeling and study the migration processes of various poorly and highly sorbed pollutants, including radionuclides that flow into the waters.

We modeled the pollution processes for the groundwater, especially for the confined ones, using the MT3D mathematical model, while taking into account 3 possible scenarios of contamination: 1) with highly sorbed pollutants, 2) with highly sorbed pollutants, including the radioactive ones, 3) with poorly sorbed pollutants.

To study the pollutants migration in the model, we selected two profiles along with some individual sites. We assessed the ecological condition of groundwater, watershed layer and confined waters.

The modeling allowed us to compare all scenarios and analyze the factors they were determined by. We revealed that the main factors of formation of pollutant migration were their radioactive decay, their sorption characteristics and the hydrodispersion of groundwater flows, which depended on the geological and hydrogeological conditions of the studied territory. The diffusion also played a role in their migration, albeit insignificant.

The results of this research can be used for variously scaled assessment of the ecological condition of groundwater in different territories of the country, for design and construction of fresh groundwater intakes, as well as for development and organization of groundwater monitoring in the areas that have been affected by the Chernobyl Accident.

Materials and Methods

Choosing the Object for Modeling

Geographical Position. The object of the modeling of the hydrogeological conditions, affected by anthropogenic load, is the part of the Kaluga Region that suffered from the accident at the Chernobyl Nuclear Power Plant the most. We marked the territory boundaries along the river network: the Bolva – Ovsorok – Ogar Rivers in the west and southwest, the Resseta River in the south and southeast, the Zhizdra and Dragozhan Rivers in the northeast, and the Peretesna River in the north. Some of the western and southern boundaries matched the administrative boundary of the region itself (Fig. 1).

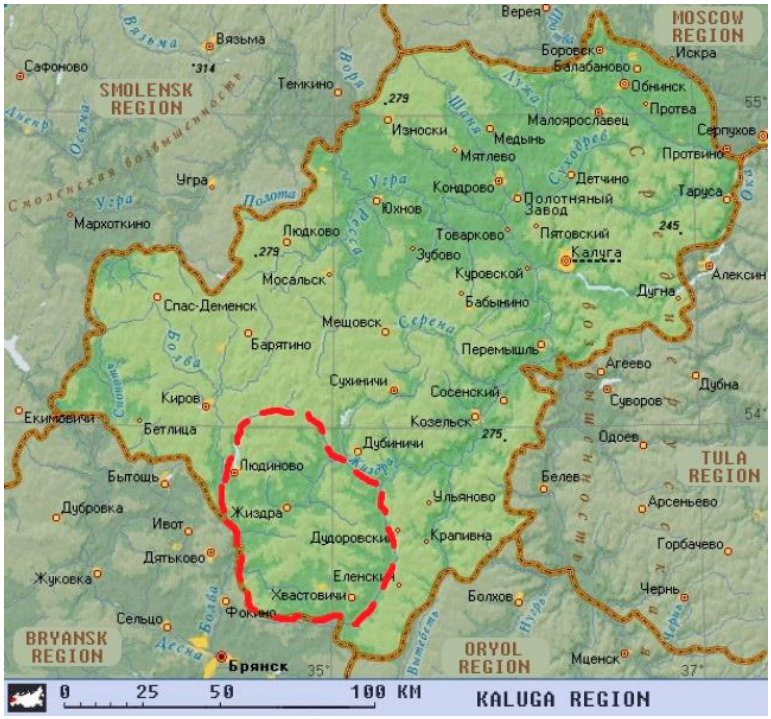

Fig. 1. Physical map of the Kaluga Region, the modeling object is marked with red line.

Hydrogeological Conditions are characterized by a wide variety of free-flow and pressure-bearing aquifers. Generally, the hydrogeological structure of the territory looks like a “layered cake”. The free-flow aquifers include waters of Quaternary (alluvial, glacial, fluvioglacial, boggy and proluvial horizons), Cretaceous and Jurassic sediments. All aquifers are connected and do not have sustained impervious horizon within the complex.

Confined aquifers of fresh groundwater consist of many interconnected Carboniferous aquifers. The Upper Jurassic impervious horizon divides these two strata (aquifer complexes), lying between them. Below the Carboniferous aquifers there are the Devonian, Proterozoic and Archean ones with salty groundwater and salt brines.

If we compare the current situation with the post-Chernobyl one, it can be said that 34 years (one half-life of radionuclides) after the accident the soil surface is still significantly polluted with radionuclides.

The groundwater monitoring (Report …, 2013; Information about …, 2013) did not reveal any aquifers with radionuclide concentrations higher than the admissible values. Unfortunately, there is no data on their concentrations that do not exceed the threshold limit value, but exceed the background values, which is important to know whenever a contamination with extremely hazardous pollutants occurs, the low doses of which have an unknown effect on public health. The monitoring was carried out mainly at the existing water intakes, meant for deeper groundwater levels, although the groundwater was not present there. Our observations in the territory of the neighboring Bryansk Region showed that the local groundwater was polluted, which allowed us to assume that the subterranean waters of the Kaluga Region, especially, the groundwater, were polluted as well.

The latest monitoring sources (Data ..., 2018; Radiation situation ..., 2019) do not list any information on groundwater.

Modeling the Processes of Geomigration of Pollutants

Describing the Conditions of Aquifers Pollution. At this stage of our research we should consider a possibility of contamination in confined water. The previous stage (Belousova, Rudenko, 2020) showed that there was a danger of radionuclides contamination due to their migration from the soil surface, which was polluted during the Chernobyl Accident, so at this stage we consider the possibility of confined water to get contamination from the polluted groundwater.

In addition, at the previous stage (Belousova, Rudenko, 2020) we analyzed the existing groundwater pollution in the Kaluga Region that revealed a presence of chemical pollution in various aquifers. All horizons from the Quaternary to the Devonian Age were subject to pollution; almost each of them contained stable strontium, barium, fluorine, nitrates, chlorides and sulfates.

At the previous stage of our research, with the help of literature sources, the pollutants were analyzed according to their classification and sorption degree. The pollutants were divided by the lowest values of the distribution coefficient (C_d), selected from the total range of the changes of the coefficient. It was done this way, because at that scale it was impossible to take into account some factors that were increasing the rate of radionuclides migration, such as microrelief, cracks and large pores. Therefore, a lower value of the hindrance factor was used to obtain the maximal values for pollution hazard, which is a common practice for geoecological researches.

In the aforementioned sources (Belousova, Rudenko, 2020) the C_d values for many chemical elements significantly exceed thousands of l/kg (C_d=152-5365 l/kg for Ni), which depends on the lithological composition of the water-bearing rocks and condition of the elements. Thus, it is difficult to classify them by the 7 degrees of pollutants sorption to solve our problem. Instead, to assess the way the confined water was protected and vulnerable to the pollutants that came from groundwater, we used a simplified concept of sorption and distinguished only 2 categories by their degree of sorption: poorly sorbed chemical elements with C_d=0-5 l/kg, and highly sorbed with C_d from 6 to 1000 l/kg (the ranges of C_d changes will be discussed below). There are almost no studies of the processes of radionuclides migration through the water-saturated stratum, and only the soils and rocks of aeration zone have been studied.

Therefore, to model the contamination processes of ground and confined waters, the following radionuclides were selected: ^{137}Cs and ^{90}Sr, along with some other highly sorbed pollutants with the

specified range of C_d, and neutral, poorly sorbed ones, such as nitrates, sulfates, chlorides and petrochemicals, which were subjected to numerical experiments in a three-layer environment.

All pollutants can be divided into groups by degree of rocks sorption. For our model a simplified classification was applied: poorly sorbed pollutants with C_d from 0 to 5 l/kg; the rest were marked as the highly sorbed ones. The subgroup of poorly sorbed included those with C_d=0.5, 1.0 and 3.0 l/kg; the highly sorbed included those with C_d=6, 26, 200 and 1000 l/kg, which characterized the sorption capacity of radionuclides ^{90}Sr and ^{137}Cs; other pollutants can also be characterized by the same values of C_d.

Our model matched a 200,000 research scale. The calculation of the pollutants migration was carried out for the first horizon of groundwater (watershed layer), which could be represented by the layers of impermeable and permeable rocks that contained the so-called "fast migration routes" of a natural and man-made origin (cracks, lenses, poorly insulated holes), and for the second horizon of confined aquifer as well.

Choosing a Computational Procedure and Model

To model the process of mass transfer in groundwater, we chose the MT3D model (Zheng, Papadopulos, 1990), which operated on the basis of the MODFLOW transport model (Anderson, Woessner, 1992). The model of the studied object was created in 2012-2013, and all the results for it are preliminary and can be found in the previous works (Belousova, 2015, 2019; Antonov, 2013).

Fundamental Mass Transfer Model MT3D

Basic Equations (Zheng, Papadopulos, 1990). A specific differential equation describes the three-dimensional mass transfer of pollutants in groundwater (Zheng, 1990):

$$\frac{\partial C}{\partial t} = \frac{\partial}{\partial x_i}\left(D_{ij}\frac{\partial C}{\partial x_j}\right) - \frac{\partial}{\partial x_i}(v_i C) + \frac{q_g}{\theta}C_g + \sum_{k=1}^{N} R_k \quad (1),$$

where C is a concentration of pollutants that were dissolved in the groundwater (g/l), t − time (day), x_i − distance along the corresponding Cartesian coordinate axis (m), D_{ij} − hydrodynamic dispersion coefficient (m^2/day), v_i − infiltration or linear velocity of water in the pores (m/day), q_g − volumetric water flow per unit of volume of an aquifer that represents a source (positive) and flow (negative) (1/day), C_g − concentration of pollutants of the variable source or flow (g/l), θ − porosity, and $\sum_{k=1}^{N} R_k$ − chemical term of the reaction (g/l·day).

If we assume that only the equilibrium linear or nonlinear sorption and the rate of an irreversible reaction of first order are involved in chemical reactions, the term of chemical reaction in the equation (1) can be expressed as:

$$\sum_{k=1}^{N} R_k = \frac{\rho_b}{\theta}\frac{\partial \bar{C}}{\partial t} - \lambda\left(C + \frac{\rho_b}{\theta}\bar{C}\right) \quad (2),$$

where ρ_b is a rock density (kg/m^3), $\bar{C}$ – concentration of pollutants that were sorbed by the porous medium ($kg_{solution}/kg_{solid}$)[2], and λ – constant of a reaction of first order (day^{-1}).

After some changes, we can get the following:

$$R\frac{\partial C}{\partial t} = \frac{\partial}{\partial x_i}\left(D_{ij}\frac{\partial C}{\partial x_j}\right) - \frac{\partial}{\partial x_i}(v_i C) + \frac{q_g}{\theta}C_g - \lambda\left(C + \frac{\rho_b}{\theta}\bar{C}\right) \quad (3),$$

where R is a hindrance factor that can be determined as:

$$R = 1 + \frac{\rho_b}{\theta}\frac{\partial \bar{C}}{\partial C} \quad (4).$$

[2] $kg_{solution}/kg_{solid}$ – ratio between the mass of pollutant in its solution phase and its mass in the solid phase. The unit is canceled afterwards, and we get a dimensionless coefficient.

The equation (3) is the main one of the mass transfer model and is connected with the flow model, including MODFLOW.

The MT3D model is based on the calculation of several processes, such as advection, dispersion, linear and nonlinear sorption and some chemical reactions of first order.

Advection. The second term in the right half of the equation (3) is $\frac{\partial}{\partial x_i}(v_i C)$. It is called an advection or forced convection, describing the transfer of pollutants that mix at the same velocity as the groundwater.

Dispersion. It is the next important process in the transfer, also known as hydrodispersion. It depends on the rate of the groundwater flow filtration, molecular diffusion and mechanical dispersion of velocities.

Source-Receiver. The third part of the equation (3) is $\frac{q_g}{\theta} C_g$. It is a source/receiver term that represents the mass, dissolved in water, or a solute itself, the mass of which is being dissolved. Receivers/sources of pollution can be classified by the area of their distribution or their specific location.

Chemical Reactions. The reactions in the MT3D model are in equilibrium and driven by the linear and nonlinear sorption, as well as by the irreversible reaction of first order, which is usually a reaction of radioactive decay or biodegradation. The more complex reactions can be added to the model, if necessary, without any modification made to the existing program.

Linear and Nonlinear Sorption. It is bound to the mass transfer between pollutants that were dissolved in groundwater (solution) and those that were sorbed on a porous medium (solid). It is generally accepted that there are equilibrium conditions between the solution and solid, and that the sorption is rather fast, compared to the groundwater movement, so it can be considered instantaneous. The functional relation between the dissolved and sorbed concentrations is a sorption isotherm, which is typically included in the transport model, using a hindrance factor.

There are 3 types of sorption isotherm that were considered in the MT3D model: linear, Freundlich and Langmuir.

The linear one assumes that the concentration of sorbed pollutants ($\bar{C}$) is directly proportional to the concentration of dissolved pollutants (C):

$$\bar{C} = C_d \mathrm{C} \quad (5),$$

where C_d is a distribution coefficient (cm^3/g).

The hindrance factor is determined as:

$$R = 1 + \frac{\rho_b}{\theta}\frac{\partial \bar{C}}{\partial C} = 1 + \frac{\rho_b}{\theta} C_d \quad (6).$$

Radioactive Decay and Biodegradation. The irreversible reaction of first order includes $\lambda\left(C + \frac{\rho_b}{\theta}\bar{C}\right)$ in the equation (3). This part is a mass loss of the dissolved (C) and sorbed ($\bar{C}$) phases of pollution that occur at the velocity constant (λ), which is usually can be expressed in terms of the half-life of the radionuclides:

$$\lambda = (ln2)/t_{1/2} \quad (7),$$

where $t_{1/2}$ is the half-life of a radioactive/biodegradable material, or the time required to reduce the concentration of radionuclides down to half of their original value.

Boundary Conditions

There are 3 types of boundary conditions: 1) the concentration changes over time, cells with active concentration; 2) the concentration is the same with a given value, cells with constant concentration; 3) no concentration, cell of inactive concentration. For our study the conditions of the first and third types were set.

Initial Conditions and Hydrogeochemical Parameters of the Computational Model. At this stage the solution to the geomigration problem was aimed at the study of the possible pollution

processes in the ground and confined waters, using various scenarios of their development.

The initial distribution of the pollutants concentration in groundwater is conventionally adopted the way it is done for the surface distribution of radioactive contamination in the Chernobyl zone in the Kaluga Region. The concentration can be expressed by g/l, Bq/l, threshold limit value (TLV) or background concentrations. In this study we use the threshold limit values (Fig. 2).

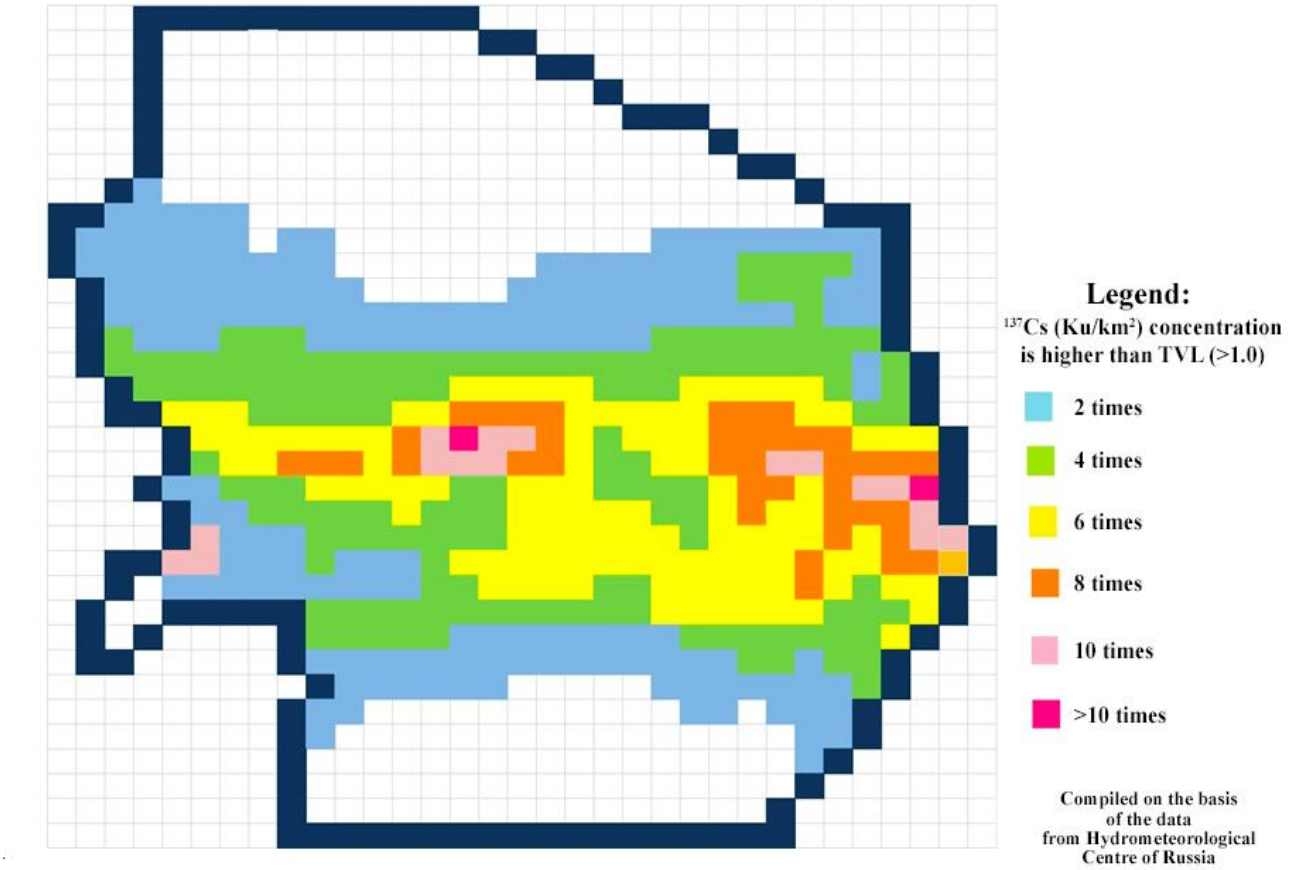

Fig. 2. Schematic map of the surface pollution with ^{137}Cs in the south of the Kaluga Region (Map …, 1991).

To study the pollutants migration in the previously composed MT3D model, we selected 2 profiles along the I-I line, from northeast to southwest of the study area, and the II-II line, from southwest to southeast, along the lines of groundwater flow, from the watershed to the discharge zone, i.e. the river (Fig. 3). Both profiles are passing through the highest watershed site No. 1 of the groundwater flow, from where the flow spreads in all directions.

The selected site is located on an elevation, shaped as a dome and fenced with rivers (Bolva, Resseta, Zhizdra) around its base, which are the reason for the complex configuration of the groundwater flow.

We analyzed the ecological situation for 4 calculated periods: 30, 60, 100 and 300 years (to link them to the half-lives of radionuclides), for 4 coefficients of sorption distribution (C_d) of pollutants: 6, 26, 200 and 1000 l/kg for radionuclides with decay and other toxic strongly sorbed pollutants without decay; and 0.5, 1.0 and 3.0 l/kg for poorly sorbed ones. We assessed the ecological situation in the first (groundwater), second (watershed layer and pore solutions) and third layers (confined waters).

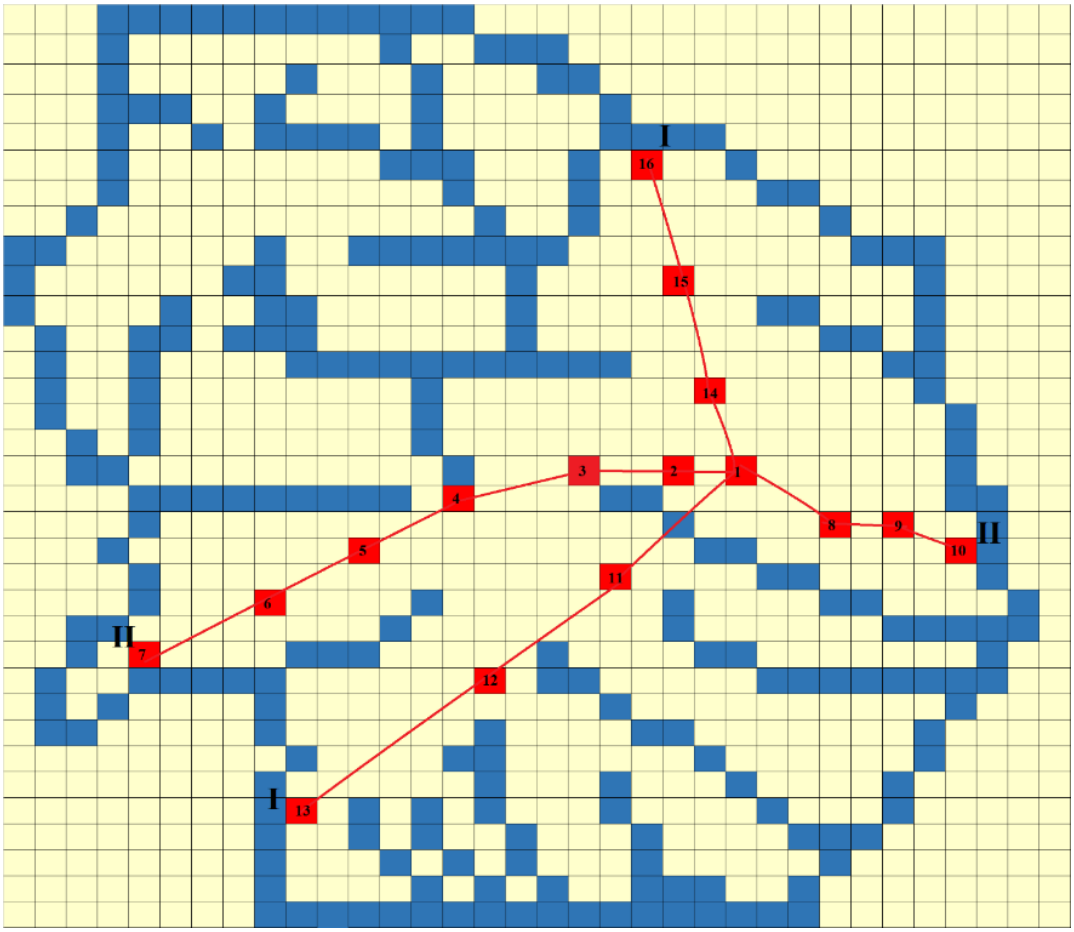

Fig. 3. Scheme of the locations with the profiles I-I and II-II, with the monitoring sites on the model of the study object.

Results and Discussion

Results of the Modeling of the Pollutants Migration from the Groundwater to the Confined Water

Scenario 1: contamination with highly sorbed pollutants without decay. Profile I-I. *30 years* after contamination (Fig. 4), the concentration is distributed as following: the amount of pollutants with C_d=200 and 1000 l/kg decreases insignificantly in the first layer – groundwater; with C_d=6 l/kg it decreases fast on the site No. 1; with C_d=26 l/kg its decrease is less significant (Table 1).

In the second layer − watershed − we registered a forming contaminated layer of pore solutions, which is at its highest at the site No. 1 with concentration reaching 1.7 TLV at C_d=1000 l/kg, while staying at 0.5 TVL in the rest of the territory. At the site No. 16, located outside the radioactive contamination zone, the very insignificant concentration is registered as well (Table 2), which indicates a spread of the contaminated zone to the neighboring territories.

In the third layer − confined waters − the separate lenses of contaminated waters are found at the site No. 11, with insignificant concentrations up to 0.1 TVL at C_d=3 l/kg. This is a sign of spot pollution.

The cartographic representation of our results is shown in the Fig. 5 as two- and three-dimensional maps. It is for demonstrative use only, since there was no way to reflect the real scale of concentration changes, especially on a three-dimensional map.

60 years after contamination, the formation tendencies of groundwater pollution remain in the

territory, but the intensity of pollution decreases. 30 years after, it is 4 TVL at C_d=6 l/kg at the site No. 1, but 60 years after it changes to 1.8 TVL; the decrease is also observed throughout the rest of the sites with different C_d values (Table 2).

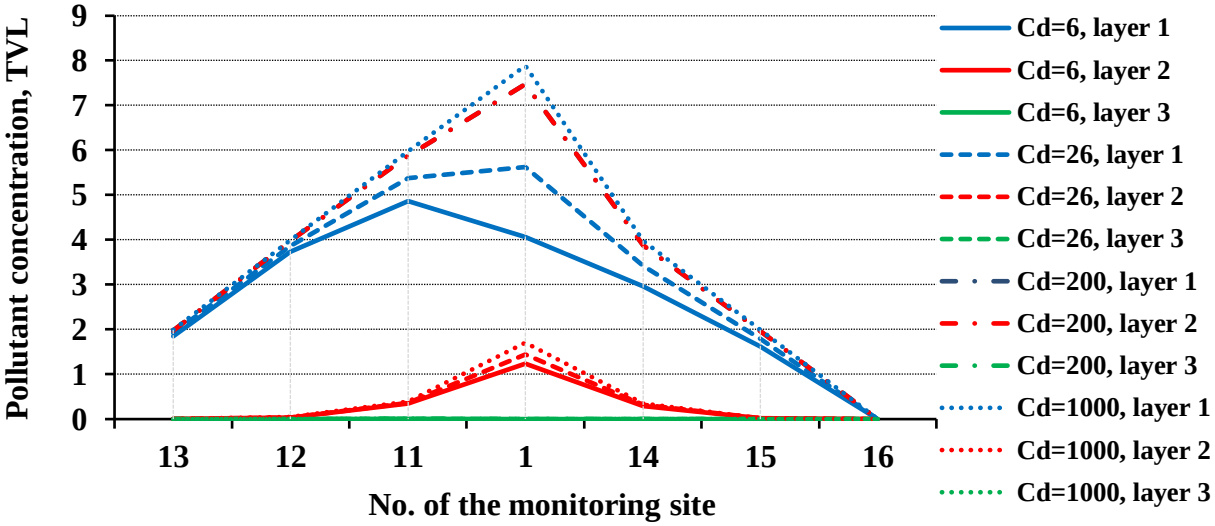

Fig. 4. Graph of the highly sorbed pollutants migration along the Profile I-I 30 years after contamination (without decay).

In a separation layer − impervious horizon − the concentrations of highly sorbed pollutant increase. Its peak is 3.72 TVL at C_d=6 l/kg at the site No. 11; and at the site No. 1 it is 3.12 TVL at other C_d values.

In the confined waters an increase is registered only at the site No. 11.

100 years after, the concentrations in the groundwater decrease down to 1.0 TVL at the site No. 1 at C_d=6 l/kg to MPC, and continues to decrease at the rest of the sites.

In the watershed layer the pollutant concentration increases. It is higher than 4 TVL at C_d=200 and 1000 l/kg at the site No. 1, and reaches 3.17 TVL (Table 2) at C_d=6 l/kg at the site No. 11.

In the confined waters the contamination is insignificant only at the site No. 11.

300 years after (Fig. 6), in the groundwater their concentration drops at C_d=6 l/kg at the site No. 1, but does not exceed 0.1 TVL; it drops significantly at other C_d values as well.

On the contrary, in the watershed layer the concentration increases abruptly up to 6.5 TVL at C_d=200 and 1000 l/kg at the site No. 1, as well as it does with the rest of C_d values (Fig. 6).

In the confined waters the contamination also spreads around, forming large lenses of poorly polluted waters (<0.1 TVL) at the sites No. 1, 11 and 14. We should also note that each site is a 2 x 2 km^2 square (Fig. 7).

Therefore, we can conclude that the impervious horizon plays a major role in pollutant migration from the groundwater to the confined ones. It reliably protects the latter from the surface and groundwater contamination, although at the same time it is also a potential source of contamination for the confined waters. Hydrodispersion has a significant effect on the migration as well.

The most important features are the type of pollutant and its sorption properties. The higher the C_d values are, the slower the pollutant will penetrate into the confined water, but the time factor reduces their chances to remain clean.

Profile II-II. Unlike the first one, this profile has a complex pollution configuration in the radioactive contamination zone. We registered a maximal initial concentration at the site No. 1,

where nothing was flowing into it from other sites, but was spreading from it over the nearby sites instead. But the concentration at the site No. 1 was not at its maximum and the surface of the initial contamination had a curved shape, which severely affected the migration on the background of hydrodispersion of the flows in all layers.

Table 1. Changes of TVL values for the highly sorbed pollutants in the groundwater, watershed and confined waters during pollutants migration.

No. of the site beg./ end	30 years			60 years			100 years			300 years		
	Layer											
	1	2	3	1	2	3	1	2	3	1	2	3
C_d=6 l/kg without decay												
1 /8	4.06	1.24	0	1.85	1.72	$2.4*10^{-2}$	1.02	1.81	0	$2.04*10^{-2}$	$4.4*10^{-2}$	6.3*10-2
11 /6	4.85	0.35	$5.51*10^{-3}$	3.78	3.72	$6.28*10^{-2}$	3.01	3.17	0.18	0.59	0.41	0.43
C_d=26 l/kg without decay												
1 /8	5.63	1.44	0	3.71	2.17	$3.04*10^{-2}$	2.61	2.77	0	0.1	0.12	0.17
11 /6	5.38	0.37	$5.7*10^{-3}$	4.72	0.70	$2.8*10^{-2}$	4.18	3.98	$7.5*10^{-2}$	1.18	1.28	0.95
C_d=200 l/kg without decay												
1 /8	7.47	1.66	0	6.89	2.93	$3.77*10^{-2}$	6.42	3.91	0	3.92	4.58	0.43
11 /6	5.87	0.39	$5.87*10^{-3}$	5.73	0.77	$3.03*10^{-2}$	5.59	1.16	$5.06*10^{-2}$	4.73	2.7	0.62
C_d=1000 l/kg without decay												
1 /8	7.89	1.7	0	7.75	3.12	$3.93*10^{-2}$	7.63	4.31	0	6.86	6.64	0.55
11 /6	5.97	0.39	$5.9*10^{-3}$	5.94	0.79	$3.07*10^{-2}$	5.91	1.19	$5.15*10^{-2}$	5.71	2.99	0.67
C_d=6 l/kg with decay												
1 /8	2.10	0.93	0	0.52	0.88	$1.64*10^{-2}$	0.14	0.63	0	$1.02*10^{-3}$	$1.02*10^{-3}$	$1.95*10^{-2}$
11 /6	2.51	0.26	$4.51*10^{-3}$	1.01	1.21	$2.79*10^{-2}$	0.33	0.47	0.06	$1.2*10^{-3}$	$2.23*10^{-3}$	$6.34*10^{-2}$
C_d=26 l/kg with decay												
1 /8	2.91	1.07	0	1.01	1.23	$1.98*10^{-2}$	0.31	0.76	0	$5.86*10^{-3}$	$7.74*10^{-2}$	$2.0*10^{-2}$
11 /6	2.77	0.27	$4.64*10^{-3}$	1.26	0.39	$1.9*10^{-2}$	0.46	0.56	$2.62*10^{-3}$	$2.59*10^{-3}$	$6.26*10^{-3}$	$9.72*10^{-2}$
C_d=200 l/kg with decay												
1 /8	3.86	1.21	0	1.84	1.56	0.02	0.71	1.44	0	$1.21*10^{-2}$	0.32	$7.09*10^{-2}$
11 /6	1.85	0.28	$4.77*10^{-3}$	1.52	0.42	$2.0*10^{-2}$	0.61	0.46	0.03	$6.66*10^{-3}$	0.325	0.13
C_d=1000 l/kg with decay												
1 /8	4.07	1.24	0	2.06	1.63	$2.45*10^{-2}$	0.84	1.53	0	$1.09*10^{-2}$	0.36	$7.71*10^{-2}$
11 /6	3.08	0.29	$4.79*10^{-3}$	1.58	0.43	$2.01*10^{-2}$	0.65	0.47	$2.69*10^{-2}$	$7.68*10^{-3}$	0.33	0.13
Poorly sorbed C_d=0.5 l/kg without decay												
1 /8	3.22	1.11	0	1.24	2.59	$2.01*10^{-2}$	0.57	1.05	0	$2.57*10^{-3}$	$6.09*10^{-3}$	$2.95*10^{-2}$
11 /6	4.53	0.4	$5.39*10^{-3}$	3.25	3.83	0.13	2.39	3.16	0.19	0.267	0.29	0.37
Poorly sorbed C_d=1.0 l/kg without decay												
1 /8	3.31	1.13	0	1.29	2.56	$2.06*10^{-2}$	0.61	1.61	0	$2.82*10^{-3}$	$7.73*10^{-3}$	$2.24*10^{-2}$
11 /6	4.57	0.34	$5.4*10^{-3}$	3.31	3.82	0.14	2.45	3.15	0.2	0.29	0.29	0.4
Poorly sorbed C_d=3 l/kg without decay												
1 /8	3.64	1.18	0	1.52	2.31	$2.25*10^{-2}$	0.76	1.69	0	$7.76*10^{-3}$	$1.94*10^{-2}$	$4.27*10^{-2}$
11 /6	4.7	0.35	$5.45*10^{-3}$	3.52	3.77	0.1	2.7	3.18	0.19	0.41	0.45	0.43
Molecular diffusion												
11 /6							2.85	3.08	0.32	0.54	0.59	0.5

30 years after contamination (Fig. 8), the radiation circuit of the polluted groundwater repeats the circuit of the initial pollutant concentration, with a smooth and insignificant decrease of it.

It reaches 4.2 TVL at C_d=6 and 26 l/kg, while mineralization is higher at the rest of C_d values.

In the watershed layer the fully contaminated pore waters form a dome at the site No. 1 at every value of C_d (up to 1.8 TVL), but at C_d=26 l/kg the concentrations reach 5.5 TVL at the site No. 3.

Table 2. Changes of TVL of the poorly sorbed pollutants in the groundwater, watershed and confined waters during their migration.

No. of the site	C_d (l/kg)	30 years			60 years			100 years			300 years		
		Layer											
		1	2	3	1	2	3	1	2	3	1	2	3
1	0.5	3.22	1.11	0	1.24	2.59	$2.01*^{10-2}$	0.57	1.05	0	$2.6*10^{-3}$	$6.1*10^{-3}$	$2.9*10^{-2}$
	1.0	3.31	1.13	0	1.29	2.56	$2.06*10^{-2}$	0.61	1.61	0	$2.8*10^{-3}$	$7.7*10^{-3}$	$2.2*10^{-2}$
	3.0	3.64	1.118	0	1.52	2.31	$2.3*10^{-2}$	0.76	1.69	0	$7.7*10^{-3}$	$1.9*10^{-2}$	$4.3*10^{-2}$
	6.0	4.06	1.24	0	1.85	1.72	$2.4*10^{-2}$	1.02	1.81	0	$2.04.*10^{-2}$	$4.4/10^{-2}$	$6.3*10^{-2}$
4	0.5	10.02	0.30	0	7.87	0.54	0	5.82	0.77	0	2.68	1.89	0
	1.0	10.06	0.30	0	7.96	0.55	0	6.20	0.78	0	1.84	1.89	0
	3.0	10.27	0.31	0	8.27	0.56	0	6.60	0.80	0	2.18	1.92	0
	6.0	10.50	0.31	0	8.65	0.57	0	7.09	0.84	0	2.87	1.60	0
11	0.5	4.53	0.34	$5.39*10^{-3}$	3.25	3.83	0.135	2.39	3.16	0.19	0.27	0.29	0.37
	1.0	4.57	0.34	$5.4*10^{-3}$	3.30	3.82	0.136	2.45	3.15	0.2	0.29	0.29	0.40
	3.0	4.70	0.35	$5.5*10^{-3}$	3.52	3.77	0.1	2.70	3.18	0.19	0.41	0.45	0.43
	6.0	4.86	0.32	$6.3*10^{-2}$	3.78	3.72	$6.3*10^{-2}$	3.0	3.0	0.18	0.59	0.41	0.43
14	0.5	2.67	0.28	0	1.97	1.45	0	1.14	1.45	0	0.14	0.47	$9.59*10^{-2}$
	1.0	2.70	0.28	0	2.01	1.44	0	1.19	1.47	0	0.27	0.51	$9.64*10^{-2}$
	3.0	2.82	0.29	0	2.08	1.21	0	1.34	1.49	0	0.25	0.82	$6.3*10^{-2}$
	6.0	2.96	0.31	0	2.24	0.45	0	1.54	1.53	0	0.38	0.81	$5.2*10^{-2}$
16	3	$5*10^{-14}$	$9*10^{-17}$	0	$4*10^{-15}$	$4*10^{-16}$	0	$1*10^{-8}$	$1.1*10^{-10}$	0	$4*10^{-3}$	$2.5*10^{-4}$	0
	6 w/o decay	$3.2*10^{-16}$	$5.6*10^{-17}$	0	$2.9*10^{-15}$	$3.1*10^{-16}$	0	$1.7*10^{-8}$	$6.7*10^{-10}$	0	$5.9*10^{-7}$	$1.6*10^{-7}$	0
	1000 w/ decay	$4.6*10^{-26}$	$3.2\cdot10^{-24}$	0	$1.9*10^{-25}$	8.7*10-24	0	5.7*10-24	$3.8*10^{-22}$	0	$4.9*10^{-23}$	$1.8*10^{-21}$	0
	1000 w/ decay	$3.7*10^{-26}$	$2.1*10^{-24}$	0	$1*10^{-25}$	$6*10^{-24}$	0	2*10-24	$1*10^{-22}$	0	$1*10^{-21}$	$7*10^{-22}$	0

In the confined waters no pollution is found within the profile.

60 years after, the pollutants concentration keeps decreasing in the groundwater at any value of C_d, and drops down to 1.9 TVL at C_d=6 l/kg at the site No. 1.

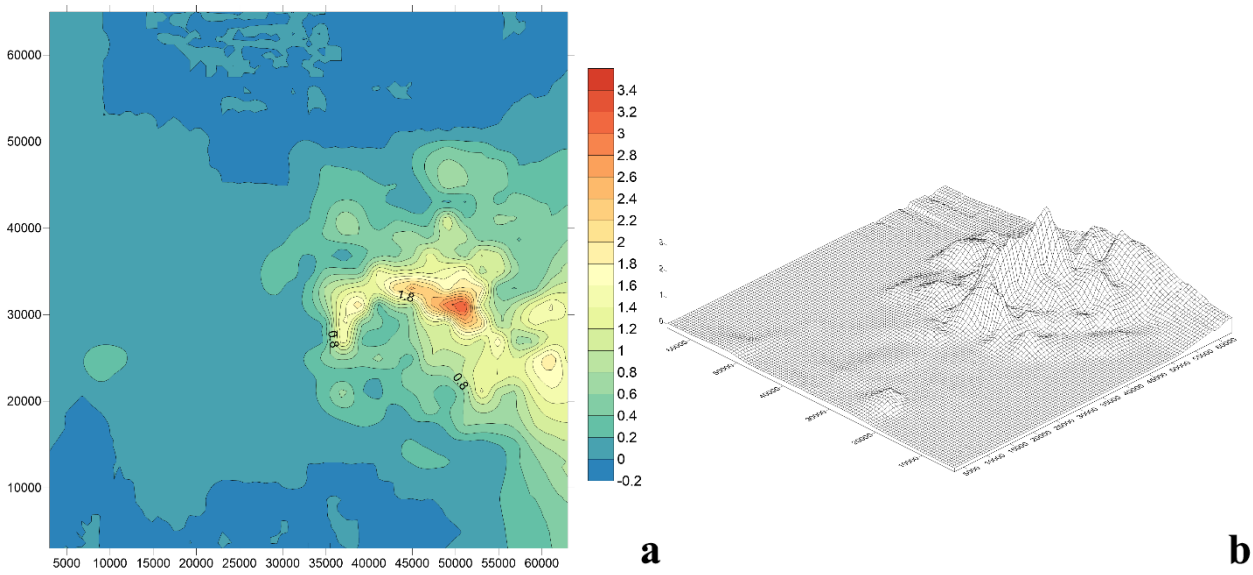

I layer

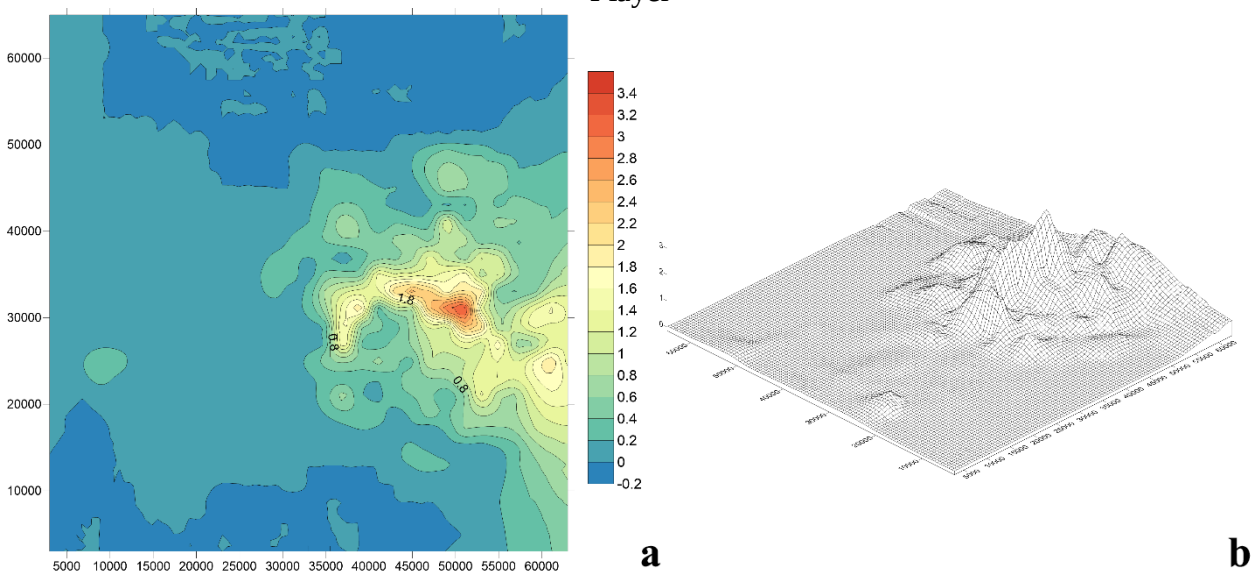

II layer

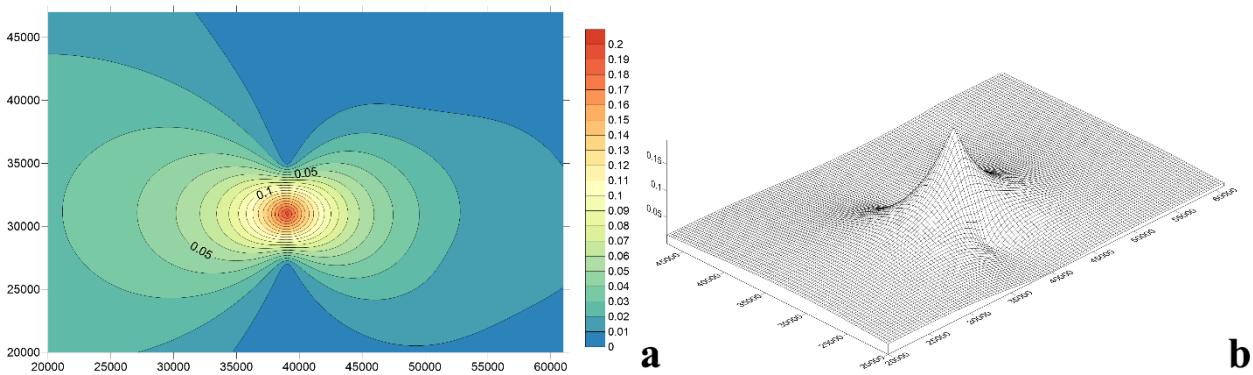

III layer

Fig. 5. Cartographic 2D (a) and 3D (b) representation of the highly sorbed pollutants migration at C_d=6 l/kg (without decay) 30 years after contamination.

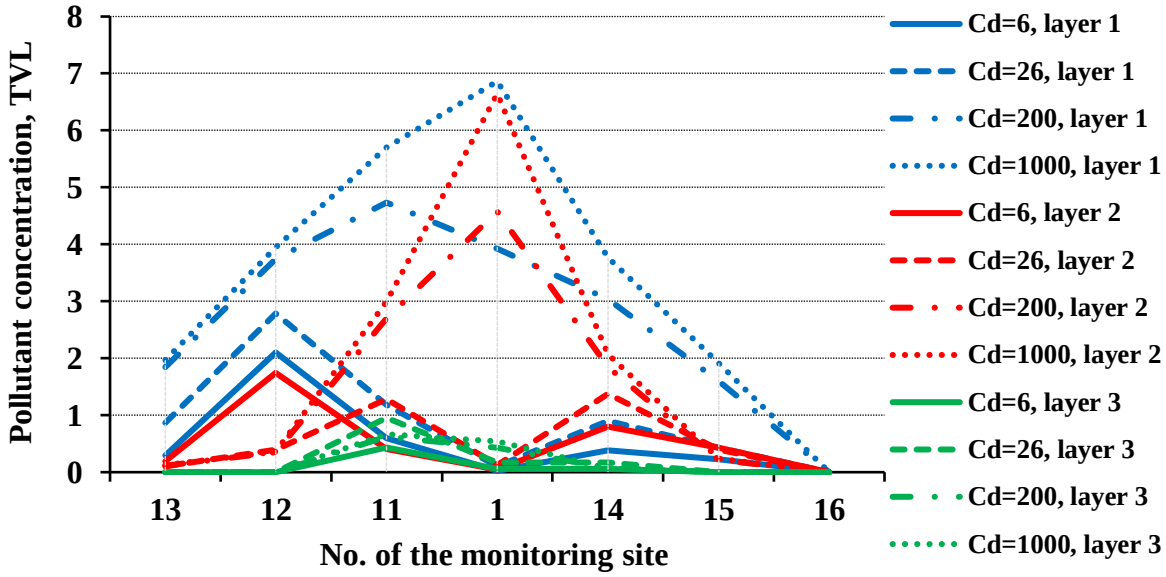

Fig. 6. Graph of the highly sorbed pollutants migration along the Profile I-I 300 years after contamination (without decay).

In the watershed layer a polluted waterlogged layer continues to form, with just one dome near the site No. 1, where the maximum is 3.1 TVL at C_d=1000 l/kg, and the minimum is 1.0 TVL at C_d=6 l/kg.

In the confined waters near the sites No. 1 and 2 a lens of poorly mineralized waters forms.

100 years after, the pollutants concentration keeps decreasing in the groundwater at the same rate and tendencies. It drops to 1.0 TVL at C_d=6 l/kg at the site No. 1.

In the watershed layer a dome of polluted pore waters also forms, with concentrations up to 4.3 TVL, covering the sites No. 1, 2, 3, 8, 9 and 10.

In the confined waters no pollution is found within the profile.

300 years after (Fig. 9), the process in the groundwater increases at the site No. 1 at C_d=6 l/kg, and its mineralization is about 0.1 TVL.

In the watershed layer the pollution decreases abruptly, reaching 8.5 TVL at C_d=1000 l/kg at the site No. 10. A second dome begins to form at the sites No. 3, 4 and 5, while the concentration is 2.9 TVL at C_d=1000 l/kg.

In the confined waters the lenses of poorly mineralized waters form near the sites No. 1, 2, 6, 8, 9 and 10.

Scenario 2: contamination with highly sorbed pollutants with decay. Profile I-I. *30 years* after (Fig. 10) the accident, the radionuclides concentration in the groundwater at the site No. 1 drops from 8.0 to 2.0 TVL at C_d=6 l/kg, while it is about 4.0 TVL at C_d=1000 l/kg.

In the watershed layer a waterlogged layer forms. The concentration at the site No. 1 is 9.8 TVL, but 1.5 TVL at C_d=1000 l/kg.

In the confined waters at the site No. 11 a lens of polluted waters forms up to 0.1 TVL.

60 years after, the concentrations decreases in the groundwater at the site No. 1 at C_d=6 l/kg down to 0.5 TVL, and 2.0 TVL at C_d=1000 l/kg.

In the watershed layer a more complicated configuration begins to form at the site No. 1, reaching 0.9 TVL at C_d=6 l/kg, and 1.2 TVL at the site No. 11. The maximal concentration is 1.5 TVL at the site No. 1 at C_d=1000 l/kg.

In the confined waters a lens of poorly mineralized waters forms at the sites No. 1 and 11.

100 years after, the concentration of radionuclides in the groundwater changes from 0.1 to 0.9 TVL at C_d=6 l/kg.

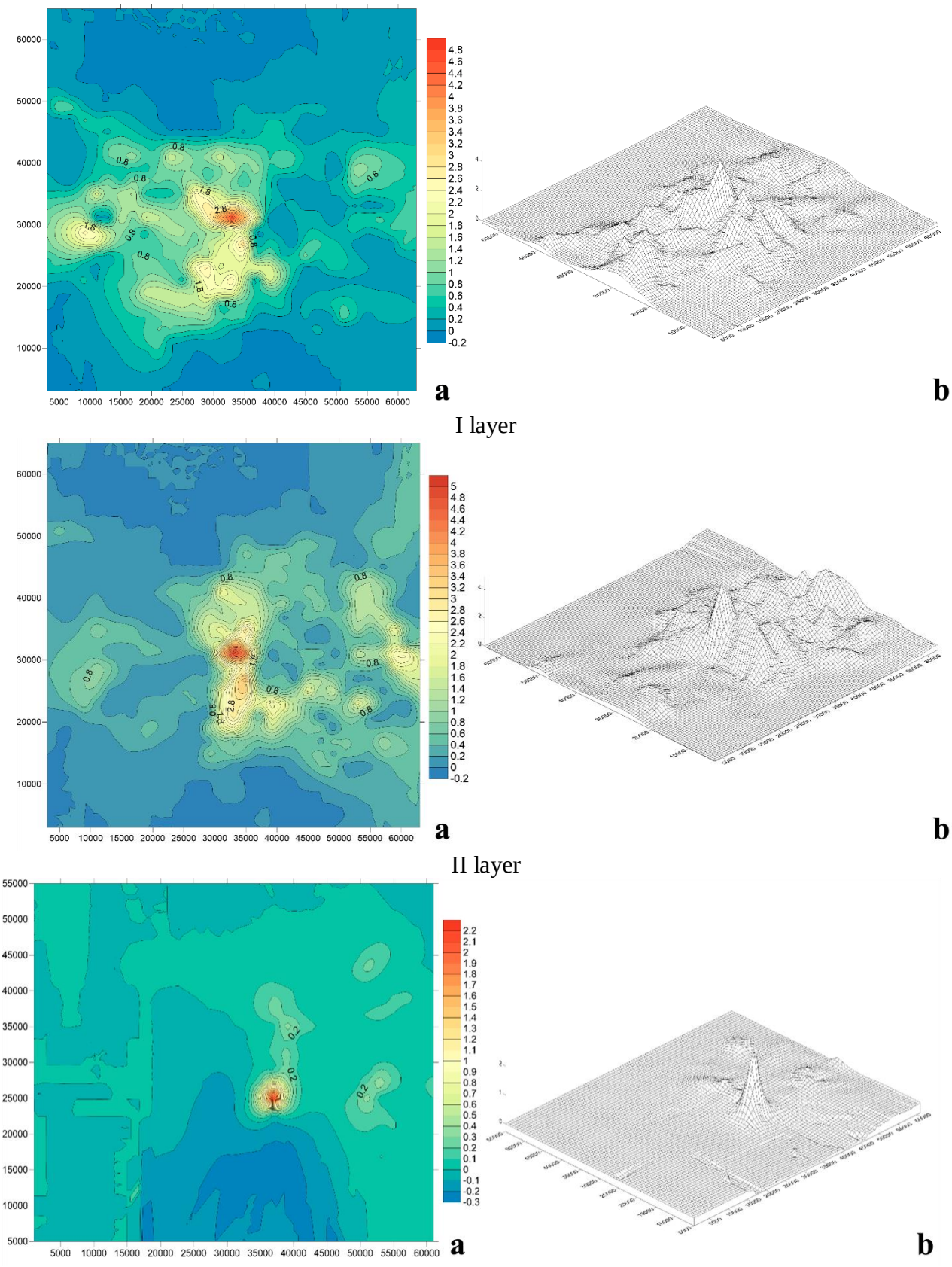

Fig. 7. Cartographic 2D (a) and 3D (b) representation of the highly sorbed pollutants migration with C_d=6 l/kg (without decay) 300 years after contamination.

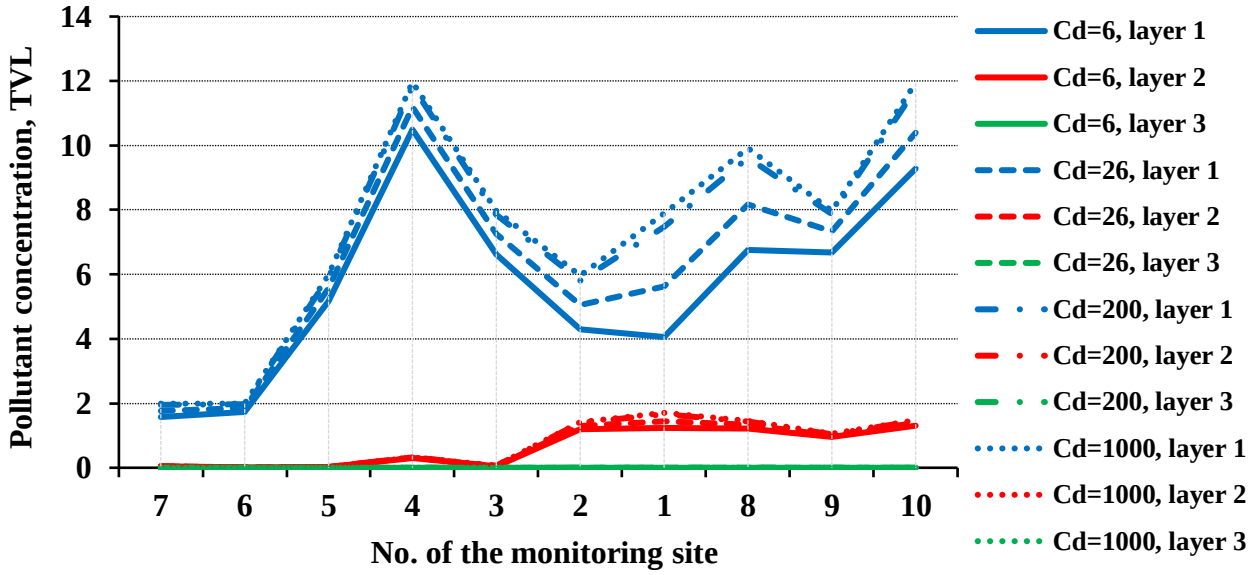

Fig. 8. Graph of the highly sorbed pollutants migration along the Profile II-II 30 years after contamination (without decay).

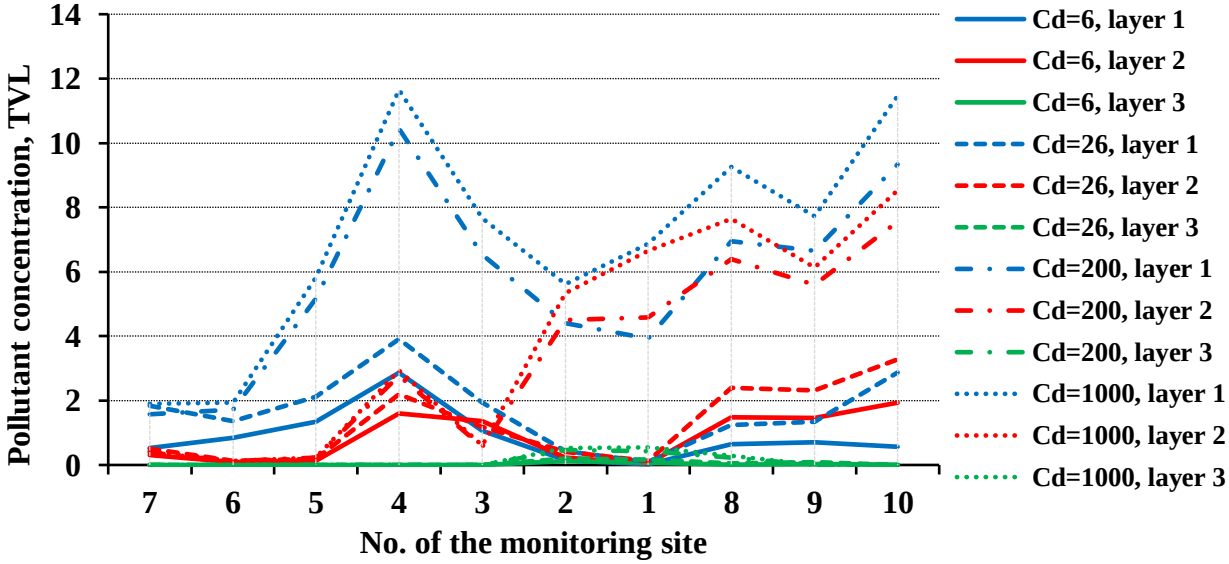

Fig. 9. Graph of the highly sorbed pollutants migration along the Profile II-II 300 years after contamination (without decay).

In the watershed layer the concentration in the dome exceeds the one in the groundwater, reaching 1.5 TVL at C_d=1000 l/kg.

In the confined waters a lens remains only at the site No. 11.

300 years after (Fig. 11), the concentration drops abruptly in the groundwater, reaching its maximum 0.001 TVL at C_d=6 and 1000 l/kg at the site No. 1

In the watershed layer it is larger than the one in the groundwater, but does not go over 0.04 TVL at C_d=1000 l/kg, with its minimum value $0.1*10^{-3}$ at the site No. 1 at C_d=6 l/kg.

In the confined waters in the lens at the sites No. 1, 11 and 13 its maximums is 0.01 TVL at C_d=200 l/kg.

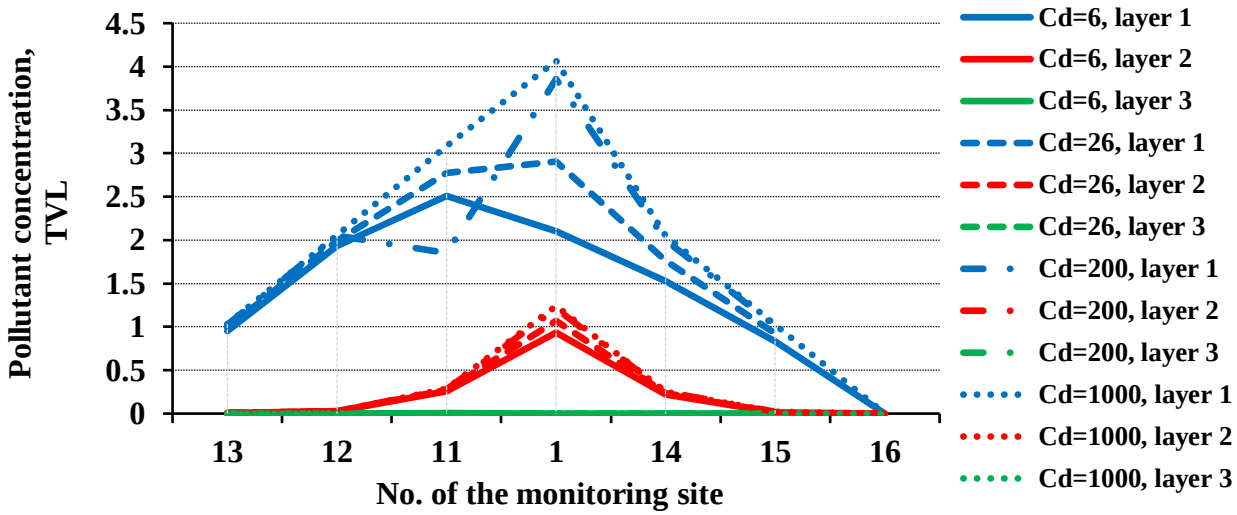

Fig. 10. Graph of the highly sorbed pollutants migration along the Profile I-I 30 years after contamination (with decay).

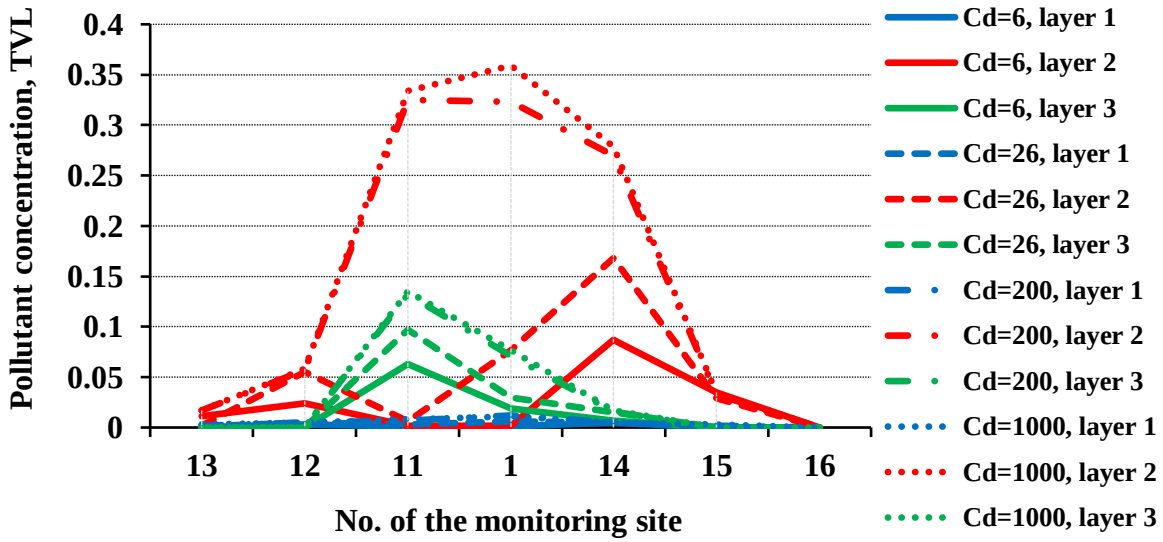

Fig. 11. Graph of the highly sorbed pollutants migration along the Profile I-I 300 years after contamination (with decay).

Profile II-II. *30 years* after (Fig. 12), the process in the groundwater is symmetrical to the initial concentration of the radionuclides. It decreases from 8.0 to 2.1 TVL at C_d=6 l/kg at the site No. 1, and from 10.0 to 5.0 TVL at C_d=1000 l/kg.

In the watershed layer the pollution of the pore waters at the site No. 1 is 0.9 TVL at C_d=6 l/kg, and 1.5 TVL at C_d=1000 l/kg. The dome of pollution stretches from the site No. 3 t0 10.

In the confined waters no pollution is found within the profile.

60 years after contamination, the concentrations decreases severely in the groundwater to 0.5 TVL at the site No. 1, with its maximum of 2.5 TVL at the site No. 4 at C_d=6 l/kg and up to 3.2 TVL at C_d=1000 l/kg. Two domes form near the sites No. 1 and 2.

In the watershed layer one dome stretches from the site No. 3 to 10, with 1.5 TVL at the site No. 1 at C_d=1000 l/kg and 0.8 TVL at C_d=6 l/kg.

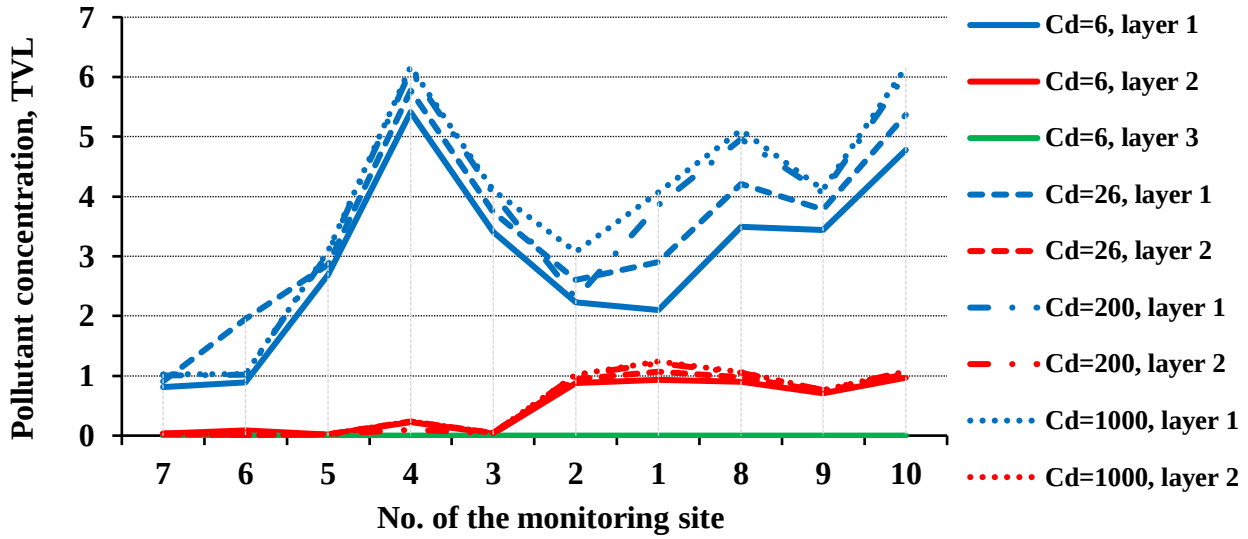

Fig. 12. Graph of the highly sorbed pollutants migration along the Profile II-II 30 years after contamination (with decay).

The cartographic schemes are shown on the Figures 13 and 14.

In the confined waters at the sites No. 1 and 2 a poorly mineralized lens forms.

100 years after, in the groundwater two domes form at the sites No. 7, 6, 5, 1 and 3. The maximal mineralization is 1.5 TVL at C_d=1000 l/kg; the minimal is 0.1 TVL at the sites No. 3, 2, 1, 8, 9 and 10 at C_d=6 l/kg, the maximal is 1.2 TVL at C_d=1000 l/kg.

In the watershed layer the mineralization of the groundwater in the first dome is insignificantly higher than in the pore waters (0.6 TVL at C_d=6 l/kg), and vice versa in the second dome (maximal concentration is 1.5-1.8 TVL at C_d=1000 l/kg, and 1.0 TVL at C_d=6 l/kg).

In the confined waters the lenses do not form.

300 years after (Fig. 15), the mineralization drops abruptly in every layer with concentration lower than 1.0 TVL. In the groundwater it grows from its minimum $0.2*10^{-3}$ at the site No. 9 to its maximum 1.5 TVL at the site No. 8 at C_d=1000 l/kg.

In the watershed layer the mineralization of the pore waters is higher than the one of the groundwater at every site. A relatively complex structure of the form has formed, with the minimal $0.6*10^{-3}$ at C_d=6 l/kg at the site No. 1 up to 0.9 TVL at the site No. 10 at C_d=6 l/kg, although the mineralization is higher along the entire profile C_d=1000 l/kg, than it is at different C_d values.

In the confined waters at the sites No. 2, 1 and 8-10 the maximal mineralization in the lenses is $0.5*10^{-2}$ at C_d=6 l/kg, as well as it is in the lens at the sites No. 1 and 2-8 at C_d=1000 l/kg.

An abrupt drop of radionuclides concentration is registered at each value of C_d. During the decay its intensity doubles, and hydrodispersion of the flow starts to play a major role as well. Generally, radioactive decay affects the migration of radionuclides much stronger than the migration of non-radioactive toxic pollutants, which can be seen clearly when the migration process is modeled according to the Scenario 1.

Scenario 3: contamination with poorly sorbed pollutants at C_d=0.5, 1.0 and 3.0 l/kg. Profile I-I.

30 years after (Fig. 16), an intense decrease of the groundwater mineralization is registered, from 8.0 TVL (initial concentration right after the accident) at the site No. 1 to 3.5 TVL at C_d=0.5, 1.0 and 3.0 l/kg at once, with very low differences in TVL values at each C_d (the lines go almost parallel to each other on the graph of the Fig. 16).

In the watershed layer the pore waters mineralization at the site No. 1 is about 1.0 TVL for each C_d value, reaching its minimum at the sites No. 13 and 16.

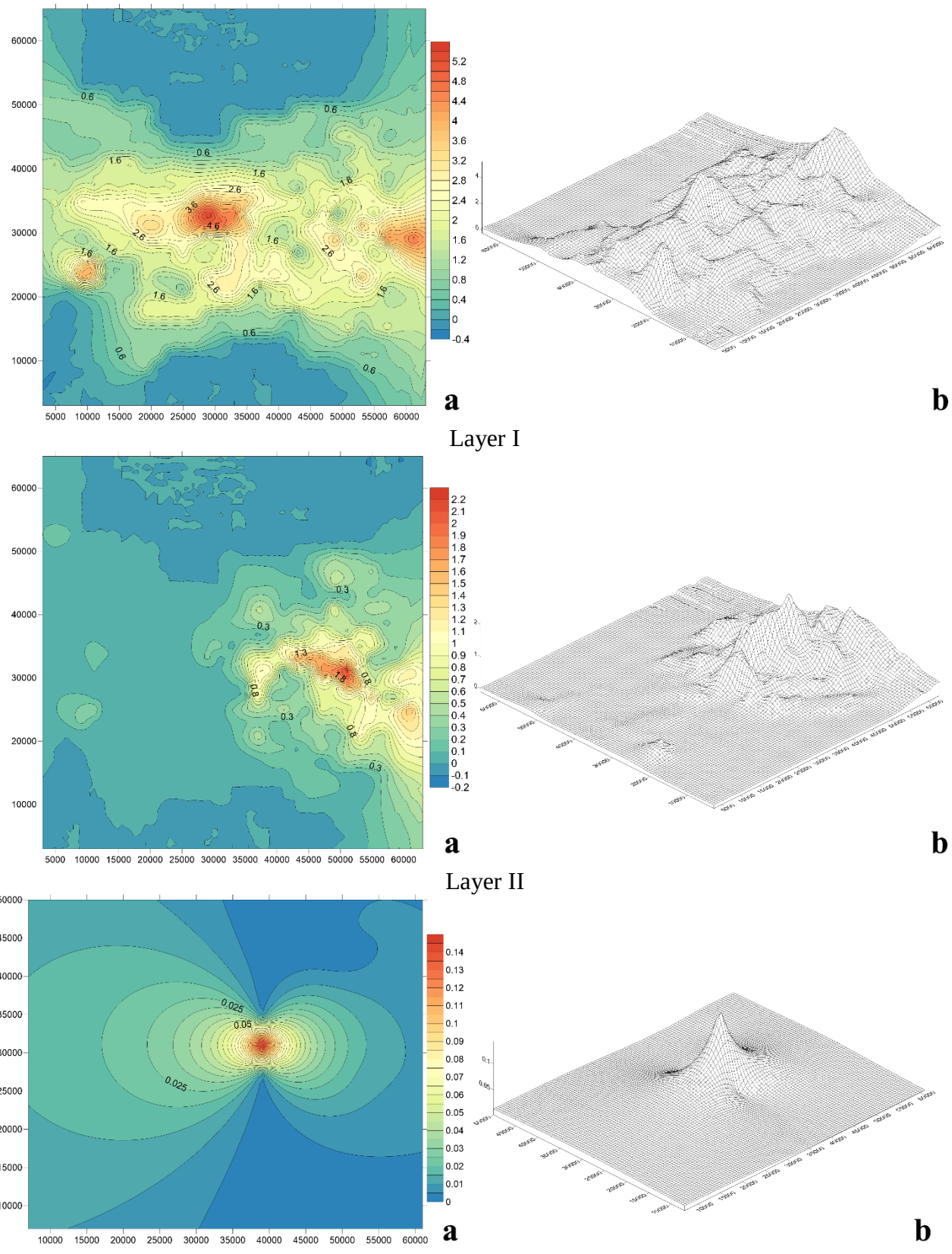

Fig. 13. Cartographic 2D (a) and 3D (b) representation of the highly sorbed pollutants migration at C_d=6 l/kg (with decay) 30 years after contamination.

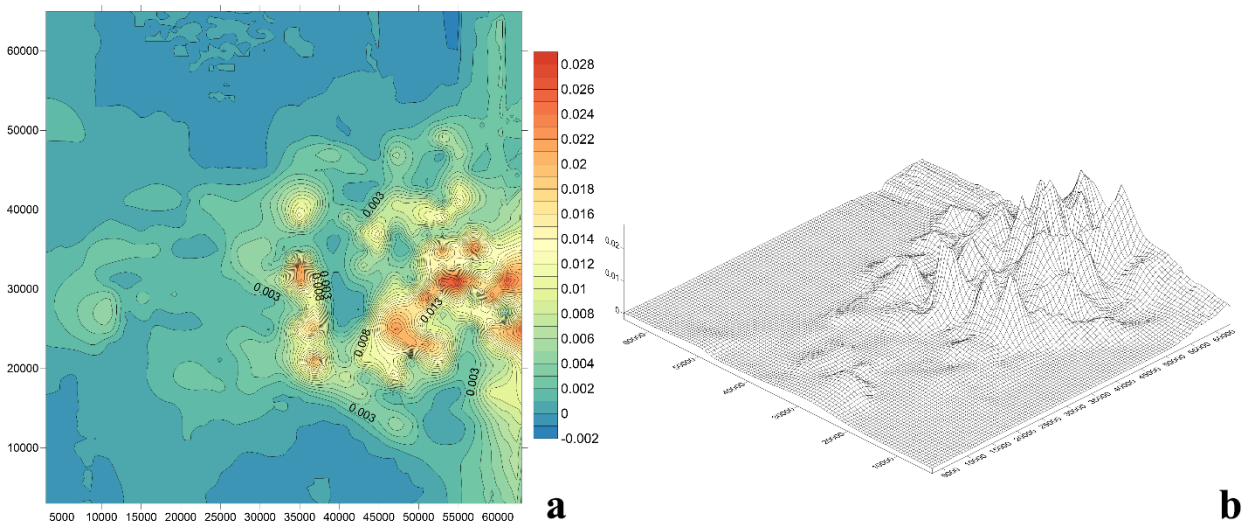

Layer I

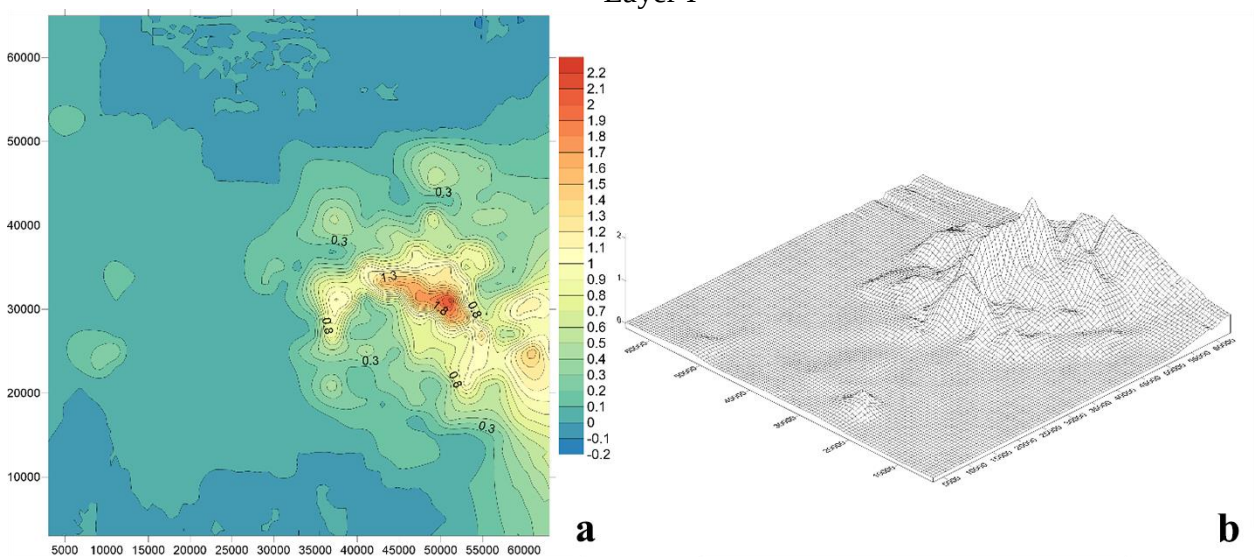

Layer II

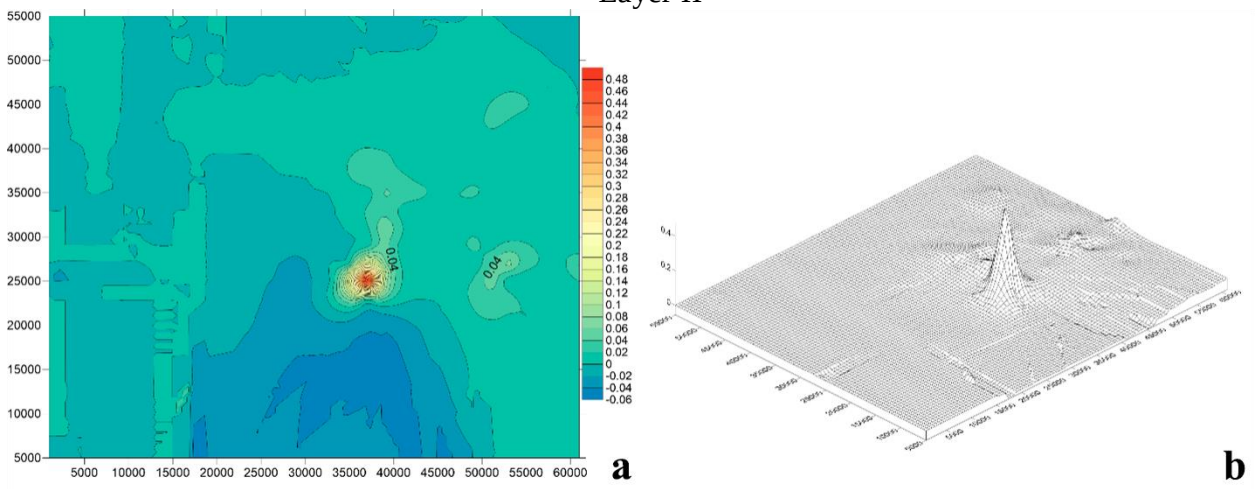

Layer III

Fig. 14. Cartographic 2D (a) and 3D (b) representation of the highly sorbed pollutants migration at C_d=6 l/kg (with decay) 300 years after contamination.

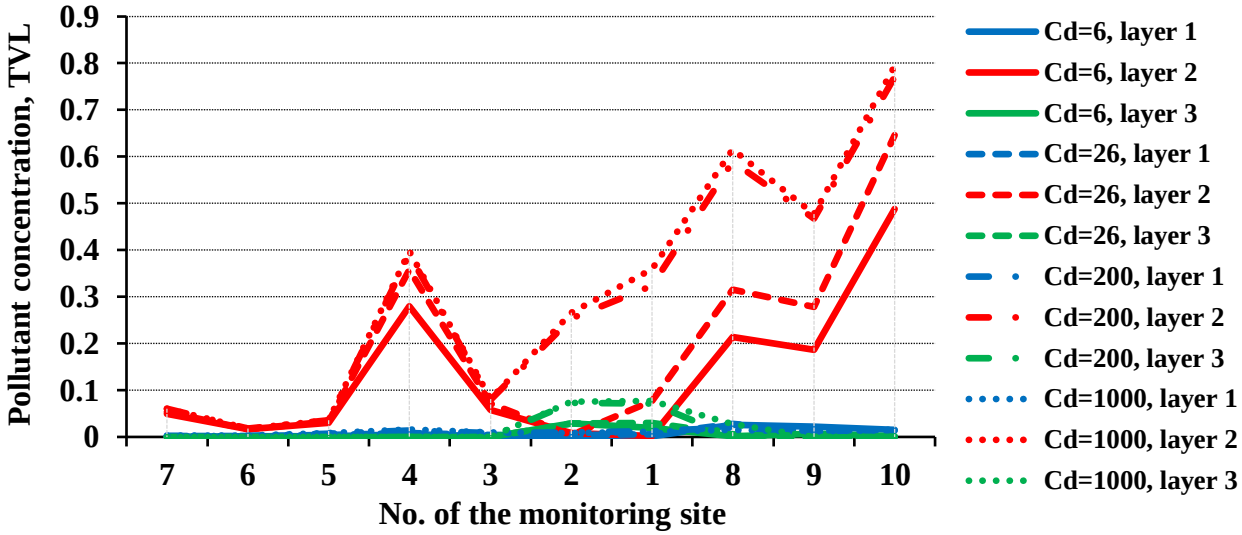

Fig. 15. Graph of the highly sorbed pollutants migration along the Profile II-II 300 years after contamination (with decay).

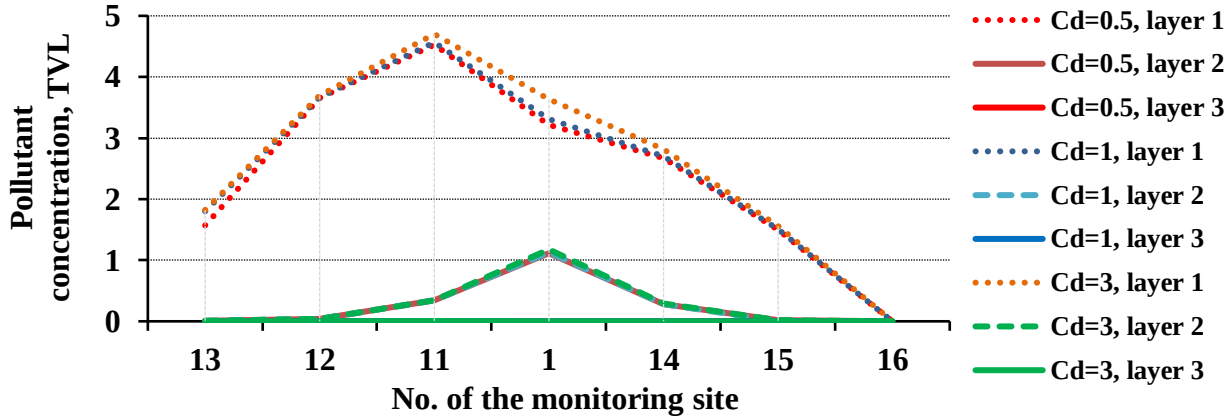

Fig. 16. Graph of the poorly sorbed pollutants migration along the Profile I-I 30 years after contamination.

A lens of polluted confined waters begins to form at the site No. 11.

60 years after, the groundwater mineralization decreases almost identically for each value of C_d, dropping down to 1.2 TVL at the site No. 1.

A dome of mineralization, growing up to 3.8 TVL, forms in the pore waters at the site No. 11 at every value of C_d.

At the sites No. 1 and 11 a lens of polluted confined waters forms with an insignificant concentration of pollutants.

100 years after contamination, the dome of polluted groundwater decreases down to 3.0 TVL at the site No. 12 at any value of C_d.

In the watershed layer the tendency remains, and the mineralization decreases down to 3.2 TVL at the site No. 11.

In the confined waters the lens of pollution spreads around.

300 years after (Fig. 17), the concentrations become almost even in the ground (maximal mineralization is <2 TVL) and pore waters.

In the confined waters a lens of poorly polluted waters forms at the sites No. 1, 11 and 14.

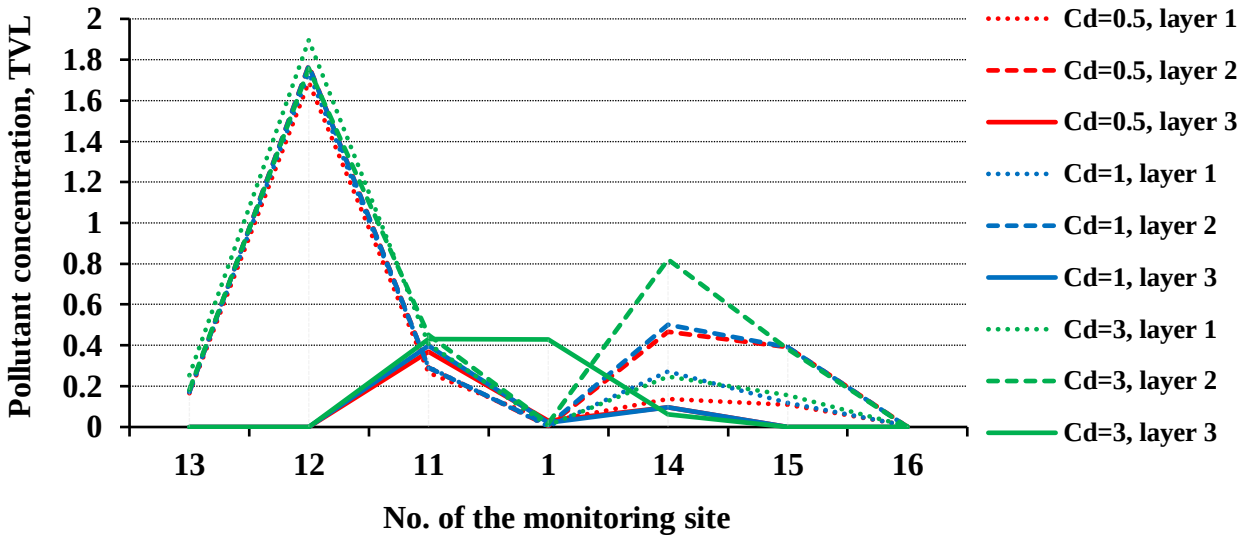

Fig. 17. Graph of the poorly sorbed pollutants migration along the Profile I-I 300 years after contamination.

Profile II-II. *30 years* after (Fig. 18), a tendency of decreasing mineralization is observed in the groundwater. The lines on the graph are parallel with the initial pollution and have almost no differences within the various values of C_d; the site No. 5 is the only one with a difference between 3.2 and 4.8 TVL at C_d=0.5, 1.0 and 3.0.

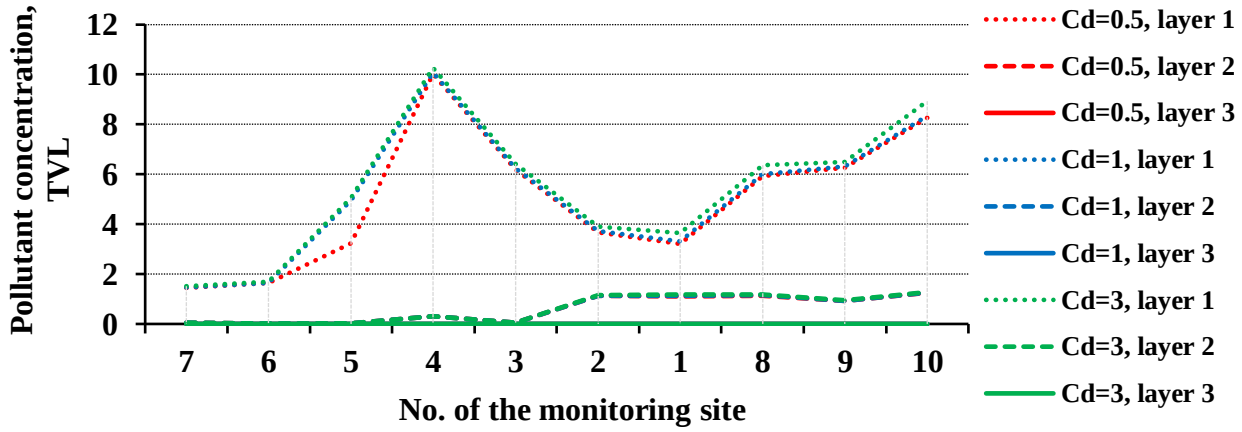

Fig. 18. Graph of the poorly sorbed pollutants migration along the Profile II-II 30 years after contamination.

In the watershed layer a poorly formed mineralization dome is found in the pore waters, almost identical to every value of C_d.

In the confined waters no pollution is found within the profile.

60 years after, the concentration continues to decrease in the groundwater.

The cartographic schemes are shown on the Figures 19 and 20.

In the watershed layer the mineralization of the pore waters increases and a dome forms at the sites No. 1, 2, 3, 8, 9 and 10, almost simultaneously, with a slight concentration differences at any value of C_d.

In the confined waters the lens of polluted waters can be found at the sites No. 1 and 2.

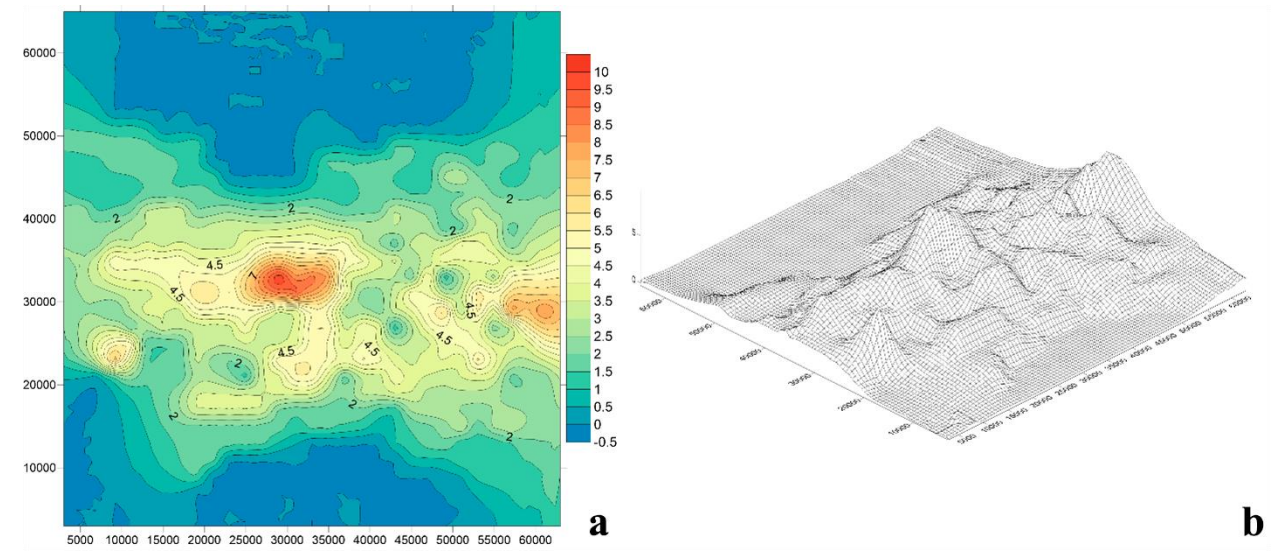

Layer I

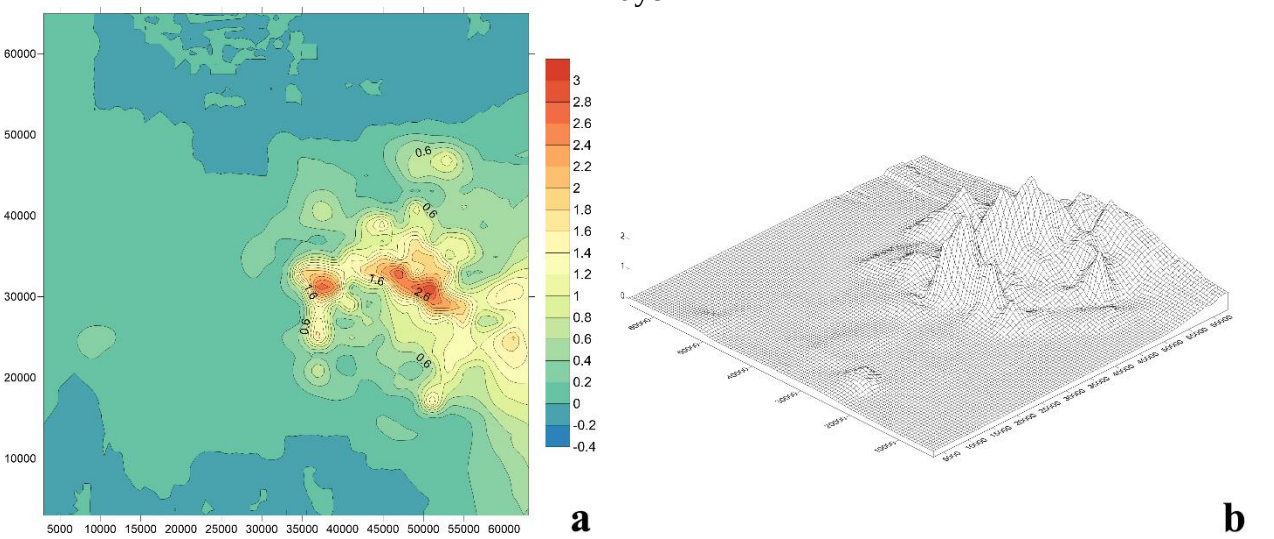

Layer II

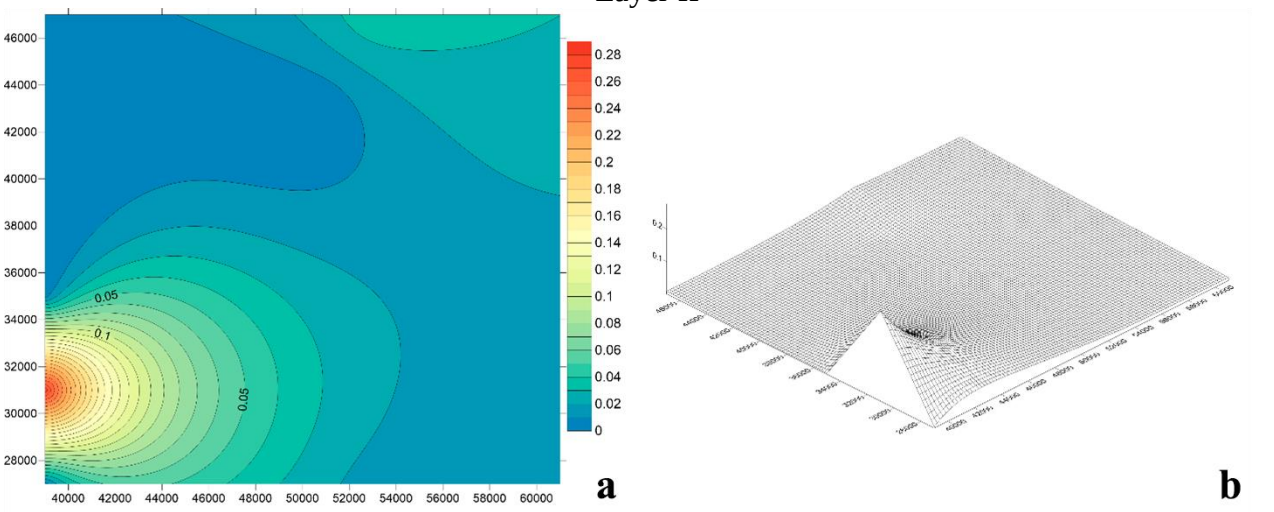

Layer III

Fig. 19. Cartographic 2D (a) and 3D (b) representation of the poorly sorbed pollutants migration at C_d=0.5 l/kg 30 years after contamination.

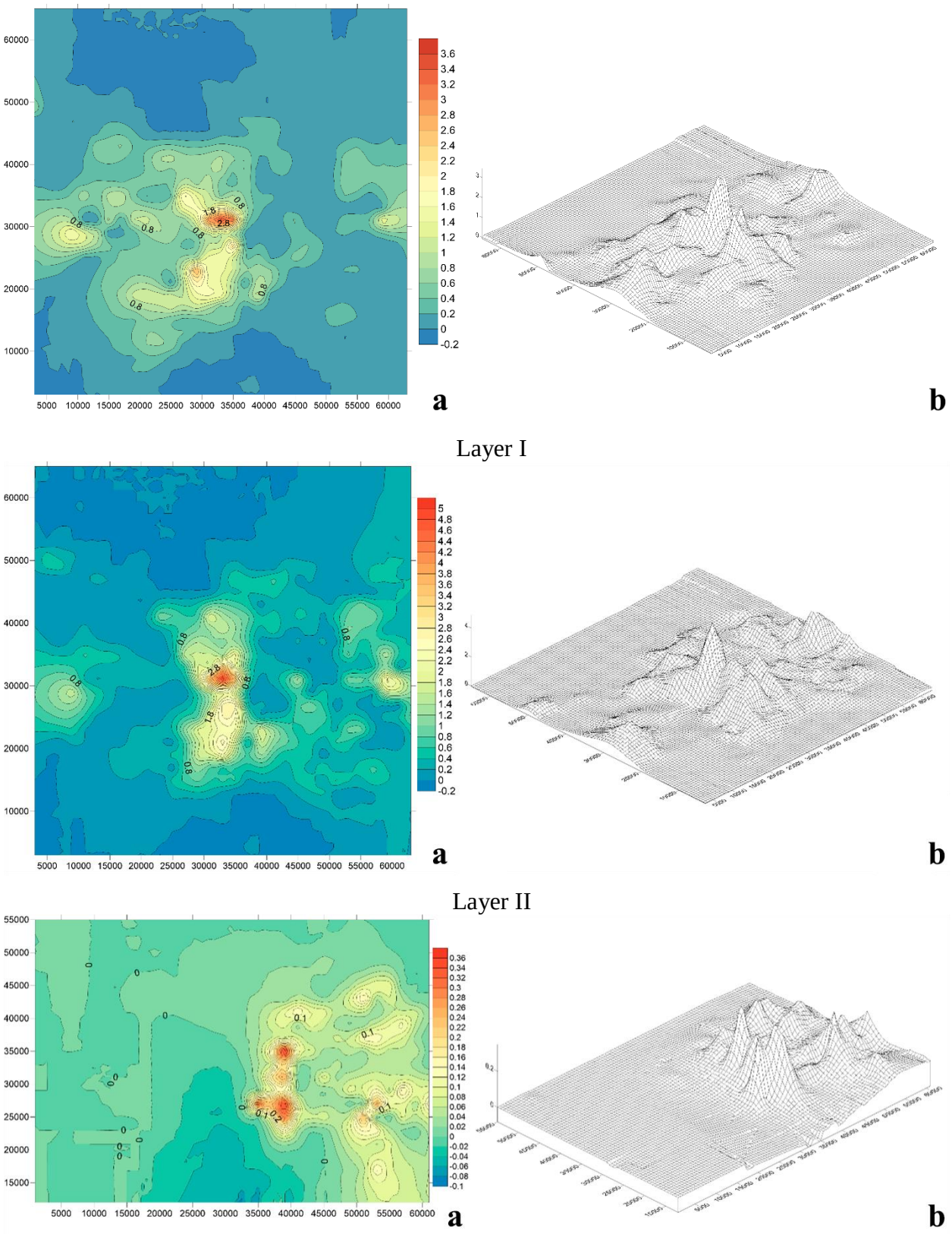

Fig. 20. Cartographic 2D (a) and 3D (b) representation of the poorly sorbed pollutants migration at C_d=0.5 l/kg 300 years after contamination.

100 years after, mineralization of the groundwater decreases, with its maximum at the site No. 4. It is almost independent on C_d.

In the watershed layer a more complex configuration of mineralized pore waters and 4 dome-like structures form, stretching from the site No. 5 to 10, reaching 3.0 TVL at the site No. 8.

In the confined waters the lens has cracked.

300 years after (Fig. 21), the mineralization evens in the groundwater, dropping down to 1.2 TVL at the site No. 4 at C_d=1 and 3 l/kg, and to 2.9 TVL in the pore waters. A couple of domes form in the ground and pore waters at the sites No. 2-5 and No. 1, 8-10.

In the confined waters two lenses of polluted waters form at the sites No. 1, 2 and 9, 10.

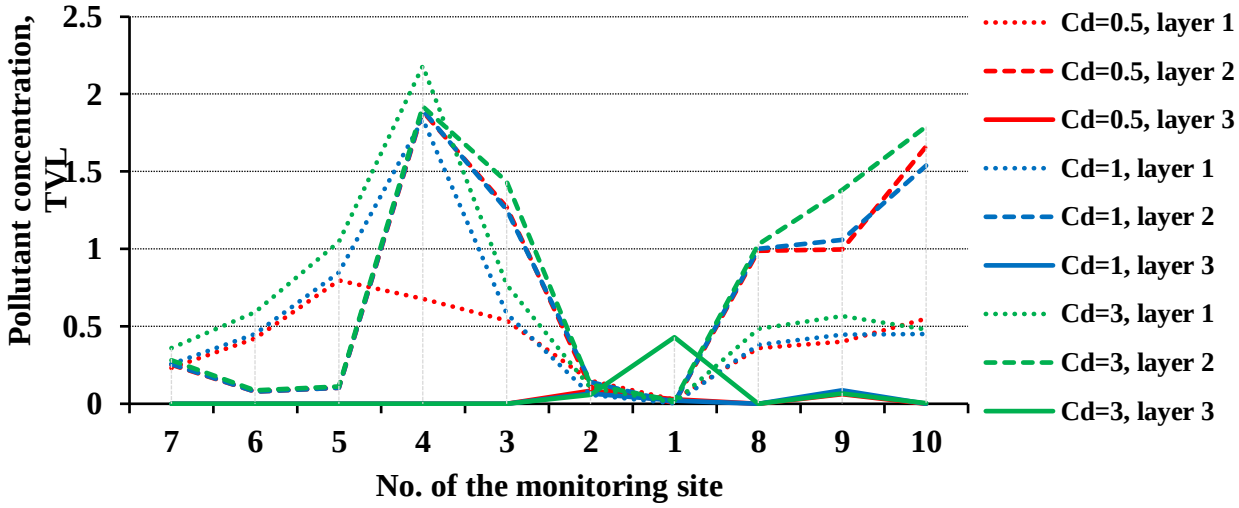

Fig. 21. Graph of the poorly sorbed pollutants migration along the Profile II-II 300 years after contamination.

We should also note that in the scenarios with highly sorbed pollutants we considered the pollutants with C_d=6 l/kg as well, which were also classified as highly sorbed. If we compare the results for that scenario and the one with poorly sorbed pollutants with C_d= 0.5, 1.0 and 3.0 l/kg, we can see that they develop symmetrically, but at C_d=6 l/kg the process slows down insignificantly. However, we classified pollutants with C_d=6 l/kg as strongly sorbed, considering that these values characterize the sorption process of some radionuclides.

Aside from the profiles, we studied the pollutants migration *at two monitoring sites*. No. 1 was a watershed site of the groundwater flow, from which the flow headed to the borderline rivers, i.e. discharge areas. On the site No. 11 a lens of polluted confined waters formed in every period of modeling, for each scenario of pollutants migration (Table 1).

Assessment of the processes of pollutants migration at these sites was carried out according to the same scenarios as it was done to the profiles.

Scenario 1: contamination with highly sorbed pollutants without decay, at the monitoring sites. *Site No. 1* (Table 1). *30 years* after contamination, the pollution of the groundwater drops abruptly from 8.0 to 4.0 TVL at C_d=6 l/kg (Fig. 22); it is intense at C_d=26 l/kg as well, but decreases gradually at C_d=200 and 1000 l/kg. *60 years* after it keeps decreasing intensely, dropping slightly even *100 years* after as well. *300 years* after it gradually decreases down to 0.1 TVL at C_d=6 and 26 l/kg, and changes from the initial 8 to 6.9 TVL at C_d=200 and 1000 l/kg (Fig. 23).

In the watershed layer an opposite process is observed. *30 years* after contamination, a pollution of pore waters forms between 1.0 and 1.7 TVL as the values of C_d increase. *60 to 100 years* after, the mineralization increases abruptly from 1.8 to 4.5 TVL as the values of C_d increase. *300 years*

after, it decreases down to 0-0.2 TVL at C_d=6 and 26 l/kg, and increases gradually from 4.6 to 6.6 TVL at C_d=200 and 1000 l/kg.

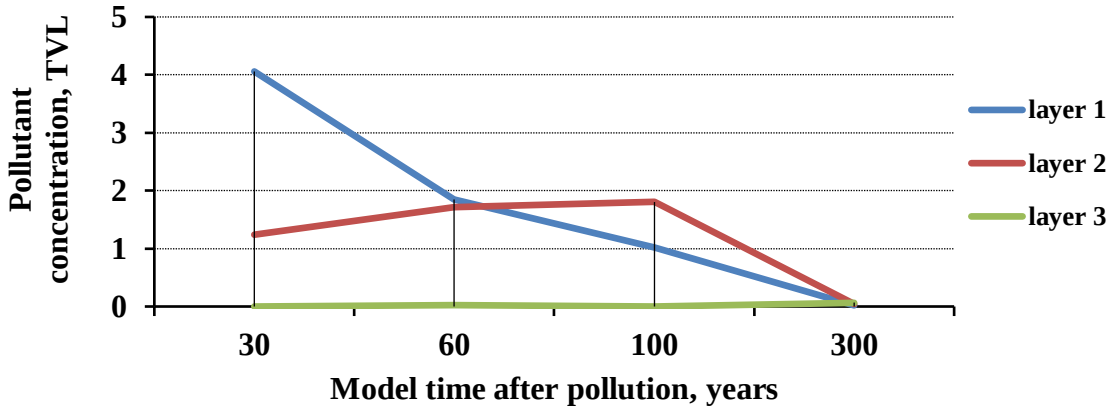

Fig. 22. Graph of the concentration changes of the highly sorbed pollutants with C_d=6 l/kg at the site No. 1.

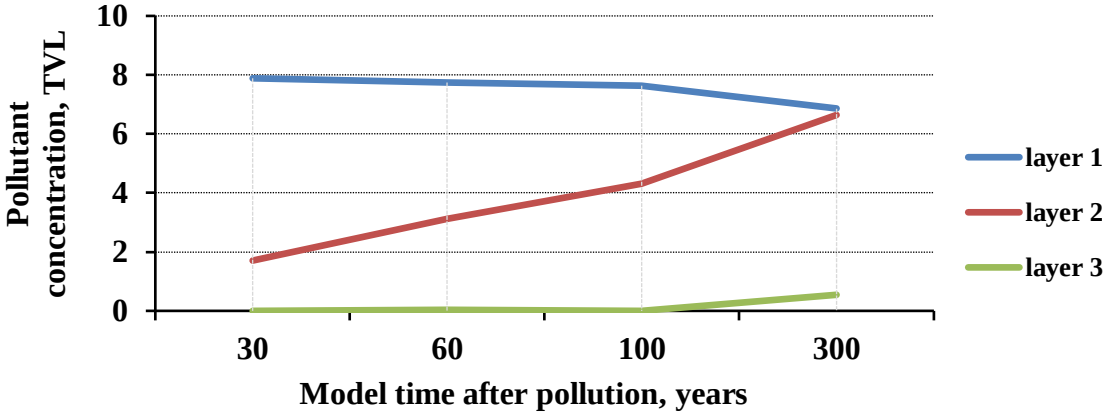

Fig. 23. Graph of the concentration changes of the highly sorbed pollutants with C_d=1000 l/kg at the site No. 1.

In the confined waters a temporary lens of poorly mineralized waters forms *60 and 300 years* after contamination.

Site No. 11 (Table 1). In the groundwater *300 years* after the mineralization decreases gradually from 6.0 to 0.6 and 1.3 TVL at C_d=6 (Fig. 24) and 26 l/kg, and increases from 4.7 to 5.6 TVL at C_d=200 and 1000 l/kg.

In the watershed layer it increases abruptly in the pore waters between *30 and 100 years* from 0.5 to 3.0-4.0 TVL at C_d=6 and 26 l/kg, decreasing afterwards up to the *300-year* period from 0.5 to 1.5 TVL. However, from *30 years to 300 years* it increases gradually in the pore waters from 2.6 to 3.0 TVL at C_d=200 and 1000 l/kg (Fig. 25).

In the confined waters a persistent lens of polluted pore waters forms, and its mineralization increases from 0 to 0.4 TVL at C_d=6 l/kg, and to 0.7 TVL at C_d=1000 l/kg.

Scenario 2: contamination with highly sorbed pollutants with decay, at the monitoring sites. *Site No. 1* (Table 1). *30 years* after contamination, the mineralization of groundwater drops abruptly from 8.0 (initial value) to 2.0 TVL at C_d=6 l/kg (Fig. 26); to 2.8 TVL at C_d=26 l/kg; and to 4.0 TVL

at C_d=1000 l/kg. It continues to drop up to the *60-year* period and *100 years* after contamination it reaches 0.2 TVL at C_d=6 l/kg, and 1.0 TVL at C_d=1000 l/kg (Fig. 27). *300 years* after the mineralization is about 0.1 TVL at every value of C_d.

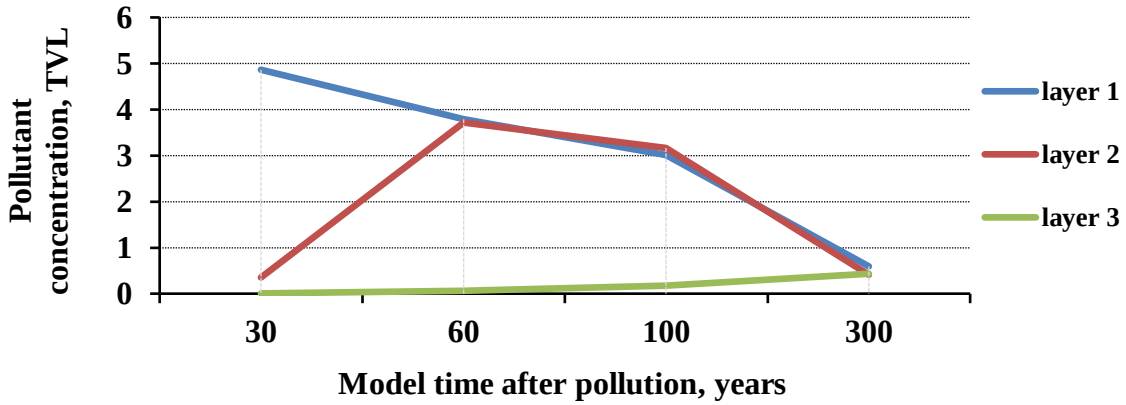

Fig. 24. Graph of the concentration changes of the highly sorbed pollutants with C_d=6 l/kg at the site No. 11.

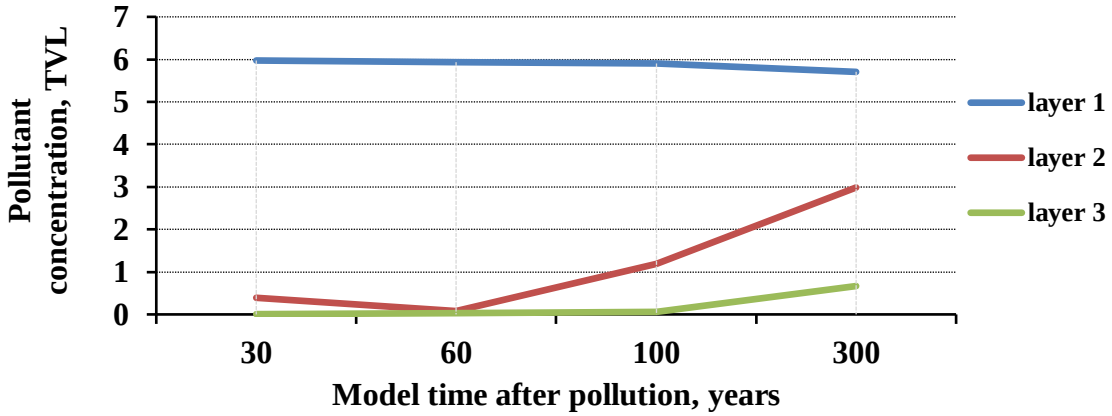

Fig. 25. Graph of the concentration changes of the highly sorbed pollutants with C_d=1000 l/kg at the site No. 11.

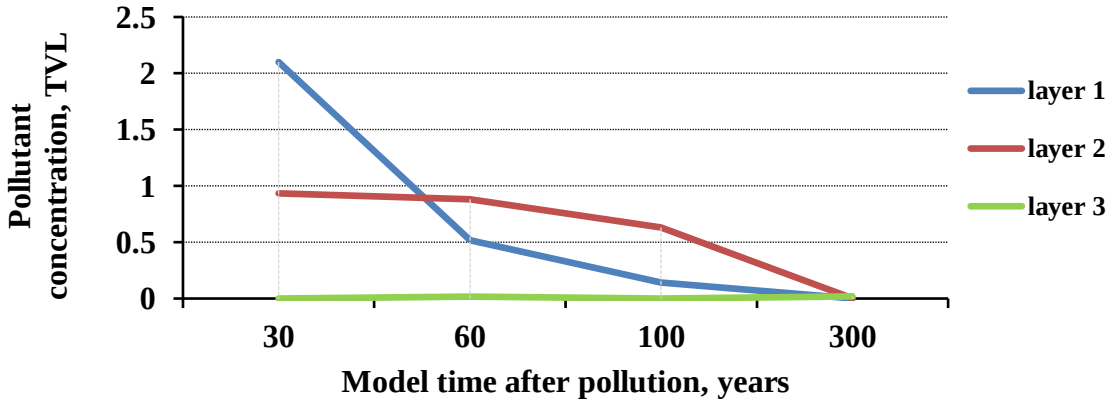

Fig. 26. Graph of the concentration changes of the highly sorbed pollutants (with decay) with C_d=6 l/kg at the site No. 1.

In the watershed layer the mineralization of pore waters increases during the period from *30 to 60 years*, reaching 0.8 TVL at C_d=6 l/kg, and 1.7 TVL at C_d=1000 l/kg. Then up to *300 years* it decreases gradually to 0.1 and 0.4 TVL at C_d=6 and 1000 l/kg.

In the confined waters a temporary lens of poor mineralization forms *60 and 300 years* after contamination.

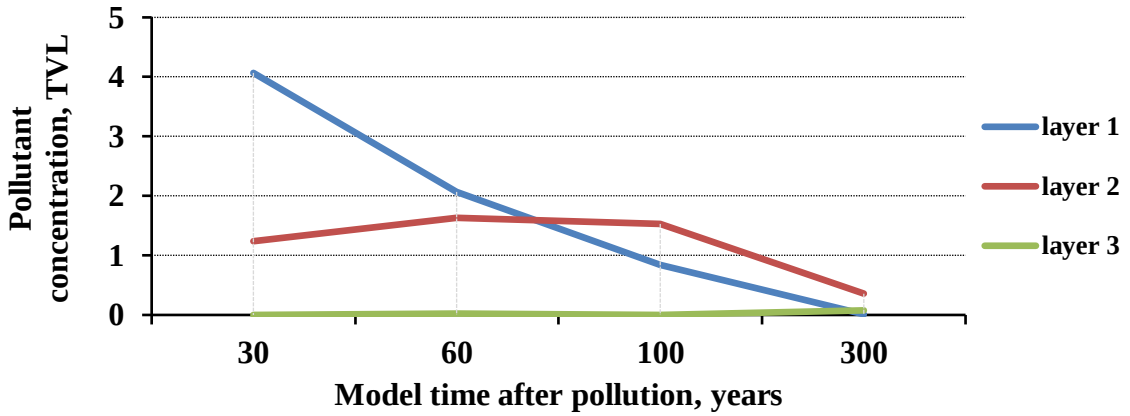

Fig 27. Graph of the concentration changes of the highly sorbed pollutants (with decay) with C_d=1000 l/kg at the site No. 1.

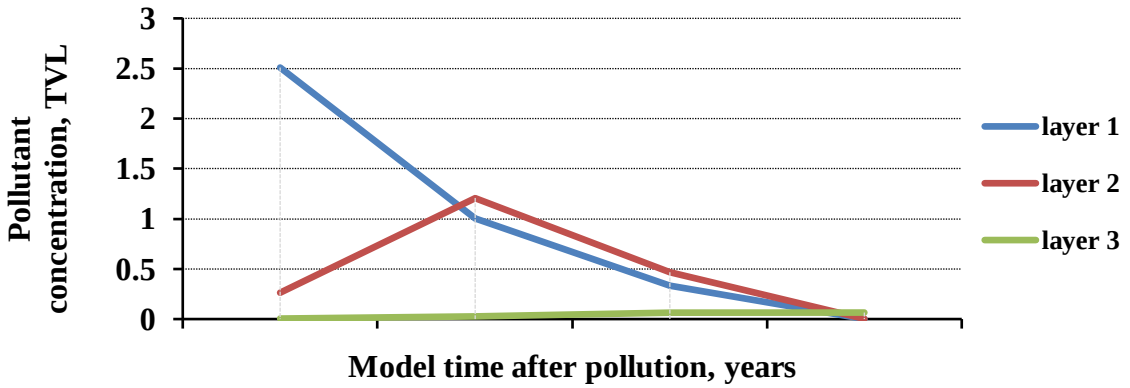

Fig. 28. Graph of the concentration changes of the highly sorbed pollutants (with decay) with C_d=6 l/kg at the site No. 11.

Site No. 11 (Table 1). From the very beginning and up to *100 years* the mineralization of the groundwater drops abruptly down to 0.3 TVL at C_d=6 l/kg (Fig. 28), and 0.8 TVL at C_d=1000 l/kg. Then, up to *300 years*, it continues to decrease gradually to 0.1 TVL at C_d=6 l/kg, and 0.4 TVL at C_d=1000 l/kg (Fig. 29).

In the watershed layer the mineralization of the pore waters increases abruptly from 0.3 TVL *30 years* after to 1.3 TVL *60 years* after at C_d=6 l/kg, then drops to 0.5 TVL *100 years* after. It stays between 0.0-0.5 TVL at any other value of C_d.

In the confined waters a persistent lens of poorly mineralized waters forms.

Scenario 3: contamination with poorly sorbed pollutants with C_d=0.5, 1.0 and 3.0 l/kg at the monitoring sites. *Site No. 1* (Table 2). From the beginning of the contamination and *100 years* after the mineralization of the groundwater drops abruptly from 8.0 (initial mineralization) to 0.6-

0.7 TVL at C_d=0.5 (Fig. 30) and 3.0 l/kg. *300 years* after it gradually decreases to 0.1 TVL at any value of C_d. *60 years* after it increases from 1.0 to 2.5 TVL at C_d=1.0 l/kg; *100 years* after the contamination it decreases to 1.0 TVL and continues to do so.

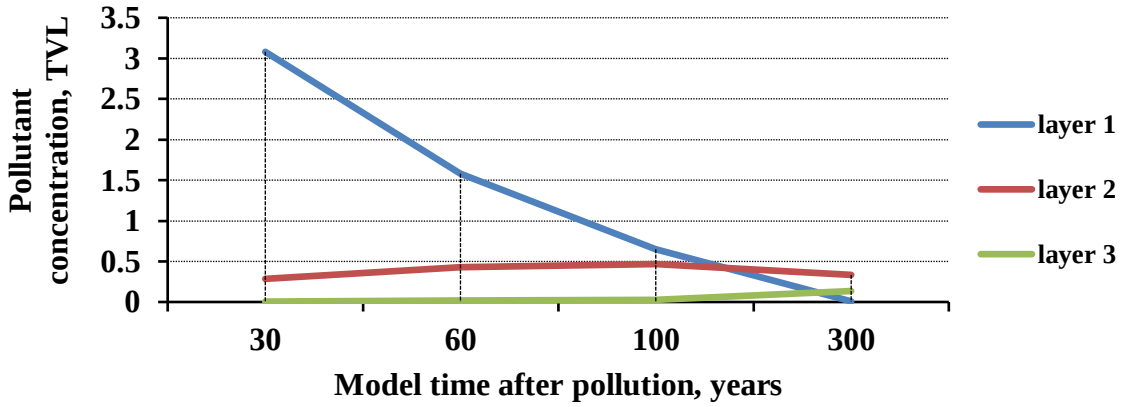

Fig. 29. Graph of the concentration changes of the highly sorbed pollutants (with decay) with C_d=1000 l/kg at the site No. 11.

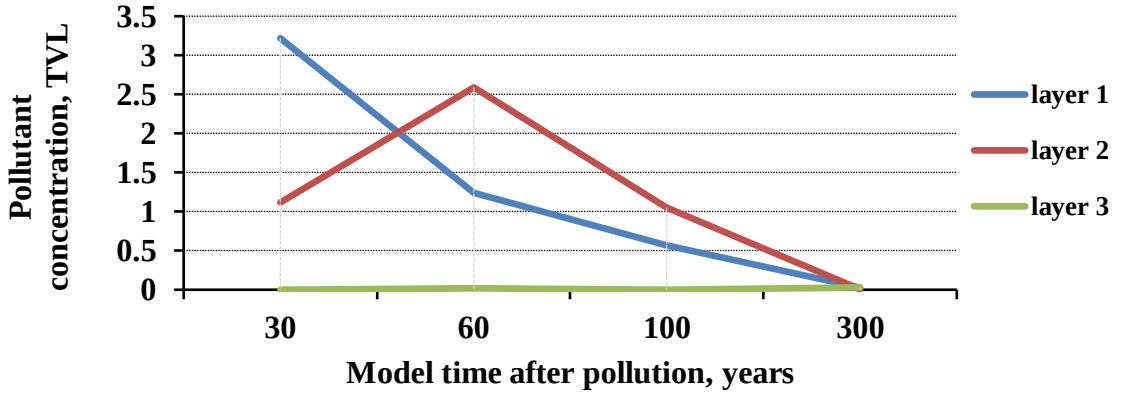

Fig. 30. Graph of the concentration changes of the poorly sorbed pollutants with C_d=0.5 l/kg at the site No. 1.

In the watershed layer the dynamics of mineralization decrease in the pore waters is the same with the groundwater at C_d=0.5 l/kg, but goes faster at C_d=1.0 and 3.0 l/kg, reaching 1.0 TVL at C_d=3.0 l/kg *100 years* after, and 0.5 TVL at C_d=1.0.

In the confined waters *60 and 300 years* after contamination an inconstant lens of poorly mineralized waters forms.

Site No. 11 (Table 2). In the groundwater at C_d=0.5 (Fig. 31) and 1.0 l/kg mineralization decreases gradually from 6.0 TVL (initial concentration) to 2.3 after *100 years*, dropping afterwards to 0.5 TVL by the *300th year*. It reaches 2.7 TVL at C_d=3.0 l/kg by the *100th year*, decreasing with time to very low concentrations (<0.1 TVL).

Comparative Characteristics of the Results, According to Various Scenarios of Pollutant Migration Development

Influence of Hydrodispersion (a transport network of groundwater flow) on the Pollutants Migration. The modeling results showed a complex flow structure in the first layer − groundwater

(Fig. 32a). It was caused primarily by the geological and hydrogeological structure of the studied and modeled territory. The territory itself is an oval elevation, located on the Kalga tectonic uplift and surrounded with external rivers, along which the boundary conditions of the first order were set on the model. Aside from the rivers, there are numerous inflows inside the territory (internal boundary conditions) (Fig. 2). All of this became a reason of the structure complexity of the groundwater flow, heavily drained by the hydrological network. Profiles I-I and II-II are confined to the watershed areas (Fig. 3). The most complex flow is located (Fig. 32a) along the horizontal boundary at 30,000-60,000 m, and the vertical one at 20,000-40,000 m.

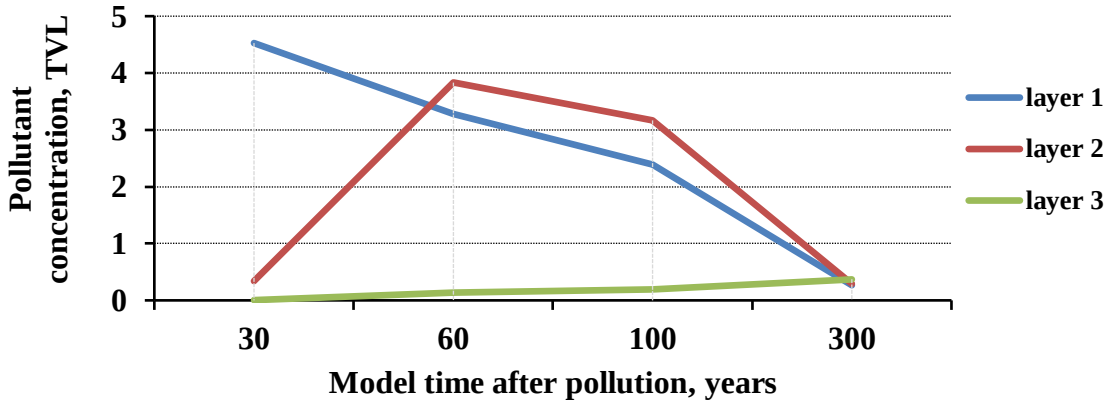

Fig. 31. Graph of the concentration changes of the poorly sorbed pollutants with C_d=0.5 l/kg at the site No. 11.

After analyzing the model results, we have found out that in the second layer − the watershed layer (Fig. 32b) − the geometry of the pore water flow is calmer, independent or almost independent on drainage of the inflows. Besides, it is located only in one square; 30,000-60,000 m horizontally and 20,000-40,000 m vertically a flow disruption, almost symmetrical to the ground flow, is registered. Apparently, a decrease in the impervious horizon thickness is also very important, enhancing the overflow that goes through it.

According to the results, we have determined that in the third layer – confined waters (Fig. 32c) – the flow structure has quite strong differences: the flow is calm, directed towards the discharge areas, to the outer boundaries, i.e. the rivers, while the internal river network has no effect on it and does not drain it. Only in one square (30,000-45,000 m horizontally, 20,000-40,000 m vertically) an area of flow disturbance has been found, inherited from the first and second layers. The main reason for this lies in a decrease in the impervious horizon thickness and formation of an area for groundwater penetration into confined waters through the impervious horizon, which happens due to the tectonic uplift in the study area and formation of a rather high watershed of groundwater.

The Influence of Sorption on the Pollutants Migration. 300 years after the accident, the concentration of the *highly sorbed* pollutants in the Profile I-I decreased significantly. Pollutants with C_d=6 and 26 l/kg accumulated in the impervious horizon, while pollutants with C_d=200 l/kg and especially 1000 l/kg remained mainly in the groundwater, although they were found in significant amounts in the impervious horizon as well, which, among other things, is controlled by hydrodispersion, a pollutant in/outflow from cell to cell (site). In the third layer – confined waters – a lens of polluted waters is forming.

In the Profile II-II a similar situation is observed, but the initial concentration in the first layer is higher than in the first profile, exceeding 10 TVL at the site No. 10, so the pollutants accumulation

in the impervious horizon is more intense as well. In the third layer two lenses are forming.

A different situation is taking place during the migration of *highly sorbed pollutants with decay* (in this case – a radioactive decay). After 300 years some traces of pollutants remain in the groundwater and impervious horizon, with C_d=6, 26, 200 and 1000 l/kg, with a concentration of 0.026-5*10^{-4} TVL, and some of them can be found in the lenses of confined waters, with a concentration of 0.027-3*10^{-20} TVL. An influence of hydrodispersion is also significant there, as the concentration in the cells does not decrease twice over 30 years, but does it instead due to the in/outflow from other cells.

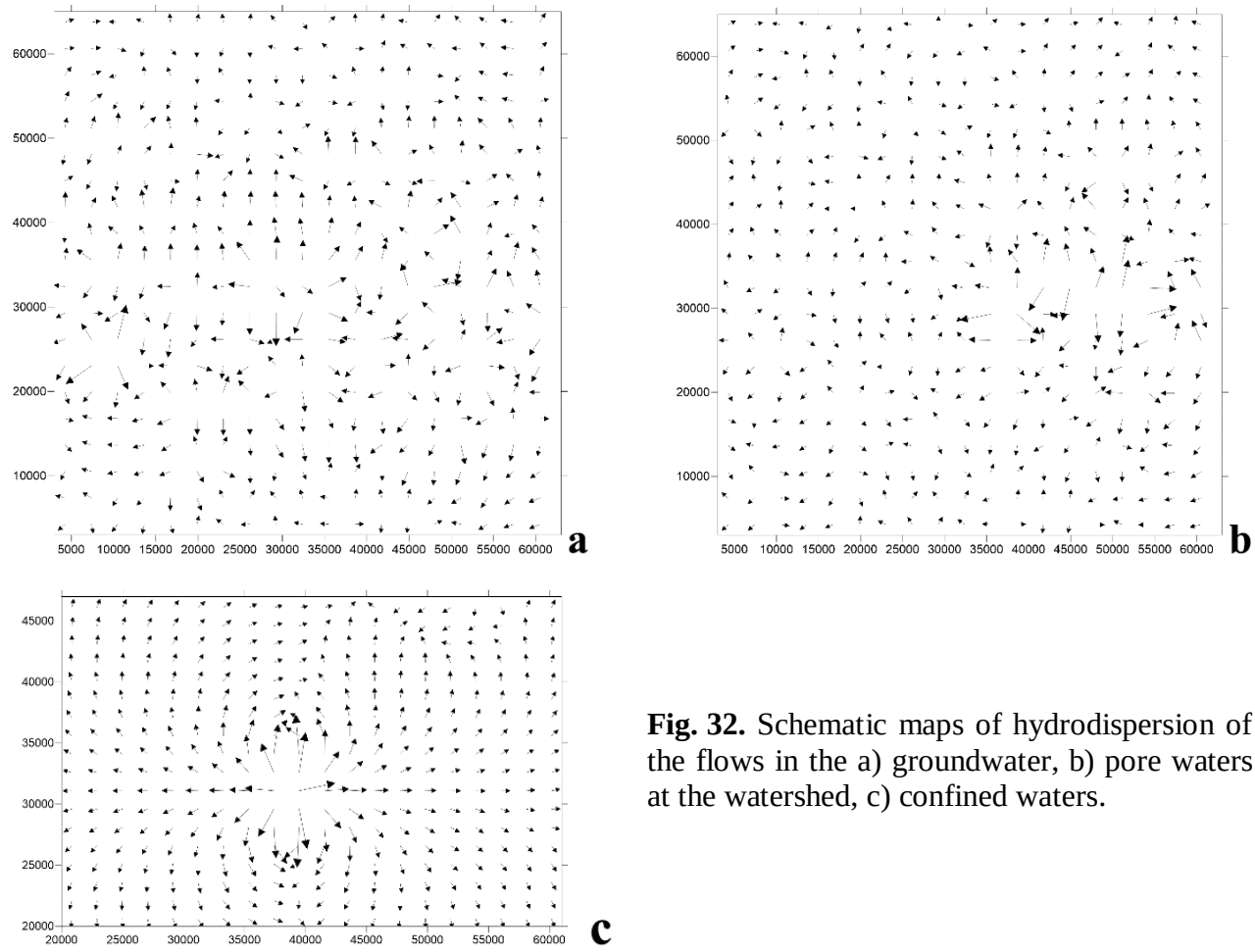

Fig. 32. Schematic maps of hydrodispersion of the flows in the a) groundwater, b) pore waters at the watershed, c) confined waters.

Poorly sorbed pollutants migrate much faster, and after 300 years their insignificant amount remains in the groundwater – 0-2.0 TVL for each C_d value, and the same amount accumulates in the impervious horizon, although sometimes it can be higher than in the groundwater. A lens of pollution is forming in the confined waters. Table 2 shows that the sorption intensity within the said interval almost does not differ at C_d=0-5 l/kg.

The main factors in the formation of pollutant migration are, first of all, decay, if there is any; secondly, their sorption properties; and thirdly, the hydrodispersion of the groundwater flows, which depends on the geological and hydrogeological conditions of the study area.

In our model we studied an impervious horizon with a consistent lithological structure, which does not always correspond to reality. The natural impervious horizons can contain lenses, layers of more permeable sediments and industrial disturbances, such as holes and other deep-lying structures. All of this can significantly disrupt the structure of the impervious horizon and accelerate

the processes of groundwater pollution. The considered situation indicates that impervious horizons cannot ensure a pollution protection of confined waters, because they have a complex permeability, which makes it possible for contaminated lenses to form in the confined waters, although in this case it happens with an insignificant concentration of pollutants.

For the analysis of the ecological situation, in addition to 2 profiles, we also selected several sites.

The sites No. 1 and 11 (Table 1) were analyzed similarly to the profiles. There the migration of various pollutants occurs according to the same trends, as it did in the aforementioned profiles.

The site No. 16 (Table 2) was placed outside the contaminated area, so we could consider the possibility of polluted ground and confined waters spreading outside the contaminated zone.

As a result we have established (Table 1) that there is a weak pollutants inflow into the first and second layers at C_d=3 and 6 l/kg, and no pollution in the third one. The inflow is sharply reduced at C_d=1000 l/kg with and without decay and is completely absent in the third layer. It increases after 300 years, reaching $4*10^{-3}$ MPC in the first layer at C_d=3 l/kg, $5.9*10^{-7}$ TVL at C_d=6 l/kg, $4.9*10^{-23}$ TVL at C_d=1000 l/kg without decay, and $1*10^{-21}$ TVL at C_d=1000 l/kg with it.

Besides, we considered the possibilities of the *pollutant diffusion process* and its influence on the pollutant migration.

The obtained results (Table 1) allowed us to reveal that over 300 years the process manifested itself in the third layer only at 22 model sites out of 1122, and only one of them (No. 11) was set within the boundaries of the analyzed profile.

Mineralization in the lenses of the third layer is from 0.1 to $5.5*10^{-5}$ TVL, while the maximal value is 0.44 TVL. It should be noted that we consider diffusion not in its pure form, but in the addition to the hydrodispersion of the flow; so, as it can be seen at the site No. 11 (Table 1), the process of formation of contaminated waters begins before a 100-year period, continuing up to the 300-year milestone. It is very close to the migration of poorly sorbed pollutants with C_d=3 and 6 l/kg, which means that diffusion, which is observed on the background of hydrodispersion, is forced. This suggests that diffusion in the area of an active water exchange depends on the strong influence of the hydrodispersion of the flows, insignificantly affecting the formation of groundwater pollution, which is formed due to other hydrogeochemical processes.

It is known that the prevailing diffusion process manifests itself in the area of hindered water exchange, where hydrodispersion is reduced to almost zero, so the diffusion takes its place instead, and its main driving force is not the gradient of the flow velocity, but the gradient of pollutants concentration.

Conclusions

For our research we chose the part of the Kaluga Region that was affected by the accident at the Chernobyl nuclear power plant the most. The results of this research are as follows.

Taking into account the three scenarios of the development of those processes, as well as various pollutants and mass transfer processes, we used the MT3D software and modeled the processes of groundwater and confined water contamination in the Kaluga region, in the radioactive contamination zone.

We also considered the possible scenarios of groundwater contamination: 1) with highly sorbed pollutants, 2) with highly sorbed pollutants, including the radioactive ones, 3) with poorly sorbed pollutants.

To study the pollutants migration in the previously created numerical model of MT3D, we selected two profiles along the lines of groundwater flow that were stretching from the watershed to the area of unloading, i.e. rivers. The ecological situation was analyzed for 4 calculation periods of 30, 60, 100 and 300 years (to link it to the half-lives of radionuclides), for 4 coefficients of sorption distribution (C_d) of pollutants: 6, 26, 200 and 1000 l/kg for radionuclides with decay and other toxic, highly sorbed pollutants without it; 0.5, 1.0 and 3.0 l/kg for poorly sorbed pollutants. We

assessed the ecological situation in the first layer (groundwater), the second one (watershed layer and pore solutions) and the third one (confined water).

Modeling resulted in all scenarios of the pollution processes development being compared with each other, and the factors that determined them being analyzed.

We found out that *hydrodispersion* affected the groundwater (first layer) the most, where a flow structure was complex due to its rather strong level of drainage. This was primarily caused by the geological and hydrogeological structure of the studied modeled territory, located on the Kaluga tectonic uplift. In the second layer (watershed) the geometry of the pore groundwater flow was calmer, independent or barely dependent on the inflow drainage. In the third layer (confined water) we registered some significant differences in the flow structure. The flow was calm and directed towards the outer boundaries, the areas of discharge, i.e. rivers; it was barely drained, while an area of the flow disturbance was inherited from the first and second layers and formed only in a small part of the territory.

We determined that *sorption* has a particularly significant effect on the *highly sorbed pollutants*. By the 300-year period their concentrations in groundwater decreased heavily, but they remained in the impervious horizon layer in large amounts, while in the confined water the lenses of polluted waters had formed.

We considered a radioactive decay for *migration of highly sorbed pollutants with decay*, which differed greatly from the above situation. After 300 years, only the traces of pollutants can be found in the groundwater, impervious horizon and lenses of the confined water.

It has been determined that *poorly sorbed pollutants* migrate more intensively, and an insignificant amount of pollutants remains in the groundwater after 300 years, while the same amount accumulates in the impervious horizon, although sometimes it can be higher than in the groundwater; besides, a lens of polluted waters has formed in the confined water.

In addition, we studied the capabilities of the process of *pollutant diffusion* and its impact on pollutant migration. It was revealed that diffusion in the area of active water exchange was under a strong influence of hydrodispersion of the streams and did not contribute significantly to the groundwater pollution, which was forming due to other hydrogeochemical processes.

Therefore, the main factors to form the processes of pollutant migration are, firstly, their radioactive decay; secondly, their sorption characteristics; and thirdly, the hydrodispersion of groundwater flows, which depends on the geological and hydrogeological conditions of the studied territory. Aside from this, diffusion plays an insignificant role in their migration as well.

REFERENCES

1. Antonov KA, Kiryakova EA, Rudenko EE. Modeling the geofiltration process in the Kaluga region (in the radioactive footprint zone) [*Modelirovaniye protsessa geofil'tratsii na uchastke Kaluzhskoy oblasti (v zone radioaktivnogo sleda)*] *Water resources, ecology and hydrological safety. VII International Conference of Young Scientists and Talented Students,* December 11-13 *[Vodnyye resursy, ekologiya i gidrologicheskaya bezopasnost'. VII ezhdunarodnaya konferentsiya molodykh uchenykh i talantlivykh studentov]*. Moscow: IVP RAS, 2013:121-125.

REFERENCES

1. *Антонов К.А., Кирьякова Е.А., Руденко Е.Э.* 2013. Моделирование процесса геофильтрации на участке Калужской области (в зоне радиоактивного следа) // Водные ресурсы, экология и гидрологическая безопасность: VII международная конференция молодых ученых и талантливых студентов, 11-13 декабря 2013 г. М.: ИВП РАН. С. 121-125.
2. *Белоусова А.П.* 2015. Оценка опасности загрязнения подземных вод как компонента окружающей среды // Вода: химия и экология. № 12. С. 31-40.
3. *Белоусова А.П., Руденко Е.Э.* 2019.

2. Belousova AP. Assessment of the hazard of groundwater pollution as a component of the environment [Otsenka opasnosti zagryazneniya podzemnykh vod kak komponenta okruzhayushchey sredy] *Water: Chemistry and Ecology [Voda: khimiya i ekologiya]*. 2015;12:31-40.
3. Belousova AP, Rudenko EE. Ecological-hydrogeological studies in the territories of European Russia affected by the Chernobyl Accident [Ekologo-gidrogeologicheskiye issledovaniya na territoriyakh yevropeyskoy chasti Rossii, postradavshikh ot avarii na CHAES] *Water Purification, Water Treatment, Water Supply [Vodoochistka, vodopodgotovka, vodosnabzheniye]*. 2019;4(136):38-56.
4. Belousova AP, Rudenko EE. Transformation of groundwater vulnerability to radioactive contamination in the Chernobyl footprint zone in the Kaluga region [Transformatsiya uyazvimosti gruntovykh vod k radioaktivnomu zagryazneniyu v zone Chernobyl'skogo sleda na territorii Kaluzhskoy oblasti] Ecosystems: Ecology and Dynamics. 2020;1(4):18-103.
5. Report on the state of natural resources and environmental protection in the Kaluga region in 2012 [*Doklad o sostoyanii prirodnykh resursov i okhrane okruzhayushchey sredy na territorii Kaluzhskoy oblasti v 2012 godu*]. Kaluga, 2013:218.
6. Map of the radiation situation in the territory of European USSR in December 1990 [*Karta radiatsionnoy obstanovki na territorii yevropeyskoy chasti SSSR po sostoyaniyu na dekabr' 1990 g.*]. *Contamination density of Caesium-137 [Plotnost' zagryazneniya mestnosti tseziyem-137.]*. Moscow: Goskomgidromet of the USSR, 1991:I-35-A.
7. Data on radioactive contamination of the territory of settlements of the Russian Federation with Caesium-137, Strontium-90 and Plutonium-239 + 240 [*Dannyye po radioaktivnomu zagryazneniyu territorii punktov Rossiyskoy Federatsii tseziyem-*

Эколого-гидрогеологические исследования на территориях европейской части России, пострадавших от аварии на ЧАЭС // Водоочистка, водоподготовка, водоснабжение. № 4 (136). С. 38-56.
4. *Белоусова А.П., Руденко Е.Э.* 2020. Трансформация уязвимости грунтовых вод к радиоактивному загрязнению в зоне Чернобыльского следа на территории Калужской области // Экосистемы: экология и динамика. Т. 4. № 1. С. 18-103.
5. Доклад о состоянии природных ресурсов и охране окружающей среды на территории Калужской области в 2012 году. 2013. Калуга. 218 с.
6. Карта радиационной обстановки на территории европейской части СССР по состоянию на декабрь 1990 г. 1991. Плотность загрязнения местности цезием-137. М.: Госкомгидромет СССР. Л. И-35-А.
7. Данные по радиоактивному загрязнению территории населённых пунктов Российской Федерации цезием-137, стронцием-90 и плутонием-239+240. 2018 / Ред. С.М. Вакуловский. Обнинск: ФГБУ «НПО «Тайфун». 225 с.
8. Радиационная обстановка на территории России и сопредельных государств в 2018 году. 2019. Обнинск: НПО «Тайфун». 324 с.
9. Справка о радиационной обстановке на территории Калужской области в 2013 году. 2013. Обнинск: НПО «Тайфун». С. 8.
10. *Anderson M.P., Woessner W.W.* 1992. Applied Groundwater Modeling (Simulation of Flow and Advective Transport). London: Academic Press, Inc. 381 p.
11. *Zheng C., Papadopulos S.S.* 1990. A Modular Three-Dimensional Transport Model for simulation of Advection, Dispersion and Chemical Reactions of Systems Contaminant in Groundwater. The United States Environmental Protection Agency, Robert S. Kerr Environmental Research Laboratory. Inc., Ada, Oklahoma. 231 p.

137, strontsiyem-90 i plutoniyem-239 + 240]. Ed. C.M. Vakulovsky. Obninsk: FSBI NPO Typhoon, 2018:225.
8. Radiation situation in Russia and neighboring countries in 2018 [*Radiatsionnaya obstanovka na territorii Rossii i sopredel'nykh gosudarstv v 2018 godu*]. Obninsk: NPO Typhoon. 2019:324.
9. Information about the radiation situation on the territory of the Kaluga region in 2013 [*Spravka o radiatsionnoy obstanovke na territorii Kaluzhskoy oblasti v 2013 godu*]. Obninsk: NPO Typhoon, 2013:8.
10. Anderson MP, Woessner WW. Applied groundwater modeling (Simulation of flow and advective transport). London: Academic Press, Inc., 1992:381.
11. Zheng C, Papadopulos SS. A modular three-dimensional transport model for simulation of advection, dispersion and chemical reactions of systems contaminant in groundwater. The United States Environmental Protection Agency, Robert S. Kerr Environmental Research Laboratory. Inc., Ada, Oklahoma, 1990:231.